Title
SIMPLE ESTIMATES FOR FERMI JETS

Authors
Mohring, K.
Seiatecki, W.J.
Zielinska-Pfabe, M.

Publication Date
1984-10-01

Lawrence Berkeley Laboratory
UNIVERSITY OF CALIFORNIA

Submitted to Nuclear Physics, B

SIMPLE ESTIMATES FOR FERMI JETS

K. Möhring, W.J. Swiatecki,
and M. Zielinska-Pfabe

October 1984

Prepared for the U.S. Department of Energy under Contract DE-AC03-76SF00098

DISCLAIMER

LBL-17919

Simple Estimates for Fermi Jets*

K. Möhring,[+] W. J. Swiatecki
and M. Zielinska-Pfabe[++]

Nuclear Science Division
Lawrence Berkeley Laboratory
University of California
Berkeley, California 94720

This work was supported in part by the Director,
Office of Energy Research,
Division of Nuclear Physics of the Office of High Energy and
Nuclear Physics of the U.S. Department of Energy
under Contract No. DE-AC03-76SF00098.

SIMPLE ESTIMATES FOR FERMI JETS*

K. Möhring,† W.J. Swiatecki and
M. Zielinska-Pfabé††

Nuclear Science Division
Lawrence Berkeley Laboratory
University of California
Berkeley, California 94720

Abstract

The phenomenon of Fermi jets is investigated in the approximation of two colliding potential wells filled with degenerate Fermi gases of nucleons. A model is formulated which largely bypasses the explicit treatment of the relative motion of the nuclei, assumed to be governed by the window friction mechanism. Formulae for the velocity distributions and differential cross sections for neutrons and protons jetting through either target or projectile are derived. The numerical results are investigated systematically over a wide range of nuclear reactions. It is shown that the net linear momentum carried away by Fermi jets accounts for only a rather minor fraction of the observed missing momentum in typical heavy ion fusion reactions.

*This work was supported in part by the Director, Office of Energy Research, Division of Nuclear Physics of the Office of High Energy and Nuclear Physics of the U. S. Department of Energy under Contract DE-AC03-76SF00098.

†On Leave from Hahn Meitner Institute fur Kernforschung Berlin, D-1000 Berlin-39, W. Germany

††Permanent address: Department of Physics, Smith College, Clark Science Center, Northampton, Mass 01063, USA

1. *Introduction*

It is a longstanding speculation [1–4] that in the early stages of a heavy ion collision nucleons might be emitted promptly due to an elementary addition of their Fermi velocities to the relative velocity of the colliding nuclei. The names "Fermi jets" or "Promptly Emitted Particles" (PEPs) are used to describe this phenomenon.

The presence of high-energy tails in the energy spectra of nucleons produced in nucleus-nucleus reactions has been known for a long time and theoretical interpretations in terms of "pre-equilibrium" processes have been provided. (See especially ref. [5] and references therein.) Fermi jets are a type of pre-equilibrium process, the distinguishing feature of the interpretation being the explicit use of the mean-field approximation to nuclear structure (the independent particle model) and of the macroscopic (Fermi gas) approximation, useful for not too light nuclei [ref. 6]

What could we learn from an experimental confirmation of Fermi jets?

(i) In general, the identification of Fermi jets could open up a fascinating field of investigation in which a nucleus, instead of being irradiated by a beam of nucleons from an accelerator, is, in effect, illuminated "from inside" by a flash of neutrons and protons originating in the vicinity of the contact point with the collision partner.

(ii) The intensities and angular and energy distributions of Fermi jets are expected to carry information on nuclear structure as well as on the character of the early stages of the collision dynamics. In particular, Fermi jets could throw light on the question concerning the type of friction responsible for the slowing down of colliding nuclei, i.e., whether the friction operates at relatively long ranges ("hard friction" [7]) or only after effective contact ("window friction" [8]).

(iii) In a number of heavy ion fusion reactions the measurement of the velocities of evaporation residues leads to the conclusion that the fused system lacks

part of the linear momentum brought into the reaction [9]. Fermi jets are one among several mechanisms that may be contributing to this loss of particles and momentum.

A number of authors [2,3,4,] investigated Fermi jets quantitatively. Yet, several years since the formulation of the Fermi-jet mechanism, an unambiguous identification of this process has not been achieved, and quantitative confrontations of theory and experiment are almost non-existent. Part of the reason for this situation is the cumbersome nature of the calculations necessary to characterize the Fermi jets, in particular the need to resort to computer integrations over the poorly understood time evolution of the collision dynamics. The present paper deals with a treatment of Fermi jets in which, through an appropriate change of the time-integration variable, the question of the time evolution of the nucleus-nucleus collision can be by-passed to a certain extent. This simplification makes it possible to present a more comprehensive survey of the expected properties of Fermi jets. Also, the predictions themselves are expected to be relatively less affected by the uncertainties associated with the collision dynamics.

2. *The Model*

The idealized model that we shall explore pictures the two nuclei as spherical potential wells filled with Fermi gases up to a Fermi energy E_F, equal to $\frac{1}{2}mv_F^2$, where m is the nucleon mass and v_F the Fermi velocity. The wells are assumed to have zero diffuseness and to have a constant depth E_F+S, where S is a typical value of the nucleon separation energy. (The constancy of the well depth implies that the electric forces inside the nuclei are disregarded. We will take E_F = 32.32 MeV unless otherwise stated, and S = 8-10 MeV.) The stage of the nuclear collision that is relevant for jetting starts at contact of the two potential wells. This is followed by an opening up of a window between the wells, accompanied by a slowing down of the relative motion of the nuclei. The fluxes of particles flowing both ways across the window contribute to the eventual jetting (if the

collision velocity exceeds a critical value sufficient to boost some of the particles to velocities exceeding the escape velocity) and, at the same time, cause a slowing down of the colliding nuclei by the mechanism of the window friction [ref. 8]. As the window area increases, the jetting will increase at first but, with decreasing relative velocity of the nuclei, this trend will be reversed. The jetting will stop altogether when the relative velocity has dropped below the critical value alluded to above. For collision velocities not too far above the critical value, the jetting will, in fact, be confined to a relatively short time, in which the two nuclei will not have moved much beyond tangency and—in the case of non-central collisions—the system will not have rotated by an appreciable amount. The above assumptions, together with the use of geometrical optics to follow the trajectories of the particles leading to jetting and the disregard—at first—of rescattering (absorption), defines in outline the idealized model that we shall investigate. In this model a number of results can be derived analytically and this will be done in sec. 3. This will be supplemented by numerical calculations necessary to treat absorption and to discuss a number of additional features of the jetting process (sections 4–6). Section 7 summarizes our conclusions.

3. *Derivation of Jetting Formulae*

a) *Inversion symmetry of the jetting process.*

Consider the two spherical potential wells at some instant of time soon after contact, when their relative velocity is $\vec{U}$ and when there is a window (assumed small) through which particles are being exchanged between the nuclei. In the mid-velocity frame of reference the conditions at the window correspond to the counter-streaming of two Fermi gases with velocities $\pm\frac{1}{2}\vec{U}$. [Note that, by Liouville's theorem, two gases of non-interacting particles in a time-dependent mean field (such as underlies the present model) make room for one another in phase space and there is no need—in fact it would be wrong—to make *additional* allowances for the Pauli exclusion principle. [See ref. 10.]

It is clear that in the mid-velocity frame the injection conditions are inversion symmetric as regards the two nuclei, so that to any particle entering nucleus A_1 with velocity $\vec{w}$ there corresponds a particle with velocity $-\vec{w}$ entering nucleus A_2. In our idealization, any two such particles will now follow force-free, juxtaposed straight line trajectories through the host nuclei. (The effects of electric forces, absorption, surface diffuseness, etc. which, in general, could break the symmetry between the two trajectories, have been disregarded.) We now note that it is a trivial consequence of the geometry of tangent spheres (the nuclei are assumed to have overlapped only slightly) that a straight line drawn through the point of tangency cuts the surfaces of the two spheres at the same angle *even when the spheres are unequal*. Consequently the *exit* conditions for the two particles (critical exit velocity, angle of refraction, etc.) are also inversion symmetric. It follows that the total jetting through the back sides of the two nuclei, however complicated each jetting may be as regards angular and energy distributions, will have inversion symmetry in the (instantaneous) mid-velocity frame of the colliding nuclei.

A more general way of stating the reason for this symmetry is that geometrical optics, according to which the particle trajectories are analyzed in the present idealization, is scale invariant. Thus the complete pattern of trajectories in two systems that differ only in scale are identical as regards all angles and angular distributions. The inversion symmetry for jetting would thus also hold in the case of two unequal *diffuse* potential wells that were scaled-up versions of one another (e.g., two harmonic oscillators). The symmetry *would be* broken for e.g. two Woods-Saxon wells with different radii and fixed (non-zero) diffuseness. The symmetry breaking would, however, only be in proportion to the degree that the two wells could not be approximated by a single intrinsic shape.

The above inversion symmetry simplifies the discussion in that, at any instant, jetting through only one of the two nuclei need be considered—the other

part of the jetting is obtained by inversion in the instantaneous mid-velocity frame.

b) *The Flux of Jetted Particles at Time t*

Consider again the nuclei a short time after contact (Fig. 1), when the relative velocity is $\vec{U}$. Introduce a system of coordinates moving with nucleus A_1, with the origin at the window, the z-axis along the line from the center of nucleus A_2 to nucleus A_1, the y-axis along the intersection of the scattering plane and the tangent plane, and the x-axis perpendicular to the scattering plane. The inward radial component of $\vec{U}$ is thus U_z and the tangential component is U_y. As seen from this reference system moving with nucleus A_1, the particles being injected by A_2 into A_1 are distributed in velocity space inside a Fermi sphere of radius v_F, whose center is displaced from the origin by the relative velocity $\vec{U}$ (Fig. 2). The vector sum of a particle's original Fermi-gas velocity $\vec{v}$ and the relative velocity $\vec{U}$ is the injection velocity $\vec{w}$, with tangential components (w_x, w_y) and radial component w_z. The condition for a particle injected at the window W to be jetted is that its outward radial velocity when approaching the exit point X in Fig. 1 should be greater than the escape velocity, given by w_e, where

$$\frac{w_e}{v_F} = \sqrt{\frac{E_F + S + B}{E_F}} = \eta \ , \text{ say} \ , \tag{1}$$

S being the separation energy and B the Coulomb barrier (in the case of proton jetting). Now, since the outward radial velocity at X is evidently equal to the radial injection velocity w_z, the condition for jetting is that w_z should be greater than w_e. It follows that in velocity space (Fig. 2) those particles will escape whose velocity vectors lie in a lens-shaped region to the right of the plane $w_z = w_e$. The flux of injected particles, (i.e. the number of neutrons, say, per unit area per unit time) that satisfy the escape condition will be proportional to an integral over the volume of the lens, weighted with the radial velocity component w_z. (This weighting expresses the usual enrichment of the flux in particles whose velocities are directed towards the plane across which the flux is being calculated.) The

constant of proportionality in the flux integral is most easily deduced by recalling the standard result that the one-sided (neutron) flux (i.e. the flux associated with a hemisphere in velocity space) for a Fermi gas with neutron density (ρ_n/m) and mean particle speed $\bar{v}$ $(= \frac{3}{4} v_F)$ is $\frac{1}{4}(\rho_n/m)\bar{v}$. (In conformity with ref. 8 we use ρ to denote the *mass* density.) It follows that the flux $F_1(t)$ of neutrons that at time t satisfy the condition for jetting through nucleus A_1 is (for $\eta - \nu_z < 1$) given by

$$F_1(t) = \tfrac{1}{4}(\rho_n\bar{v}/m)\,\frac{\iiint_{\text{lens}} w_z d^3v}{\iiint_{\text{hemisphere}} v_z d^3v} \tag{2}$$

$$= \tfrac{1}{4}(\rho_n\bar{v}/m)\,\frac{\int_{\eta-\nu_z}^{1}(x+\nu_z)(1-x^2)dx}{\int_0^1 x(1-x^2)dx}$$

$$= (\rho_n\bar{v}/m)(\nu_z - c)^2\left[(1+c) - \frac{c}{3}(\nu_z - c) - \frac{1}{12}(\nu_z - c)^2\right], \tag{3}$$

where $\nu_z = U_z/v_F$ and $c = \eta - 1 = (w_e - v_F)/v_F$ specifies the threshold value of ν_z below which jetting will not occur. Insofar as the inversion symmetry theorem for jetting is valid, the flux of neutrons, $F_2(t)$, that at time t satisfy the condition for jetting through nucleus A_2, is exactly the same, i.e. $F_1(t) = F_2(t)$. The total number of neutrons jetted per unit time per unit window area is $F_n(t) = F_1 + F_2 = 2F_1$.

c) *The Total Number of Particles Jetted in a Collision*

Consider first a head-on collision. The number of neutrons jetted through nucleus A_1 will be

$$\Delta N_1 = \int_0^{t_c} F_1(t)a(t)dt \quad , \tag{4}$$

where a(t) is the area of the window at time t and the integral extends from the

time of contact (t=o) to the time t_c at which the relative radial velocity has dropped to the threshold value given by $\nu_z = c$.

To evaluate eq. (4) we make use of the equation of motion (in a head-on collision) for the slowing down of two nuclei subjected to the window friction (ref. 8).

Disregarding the conservative forces (which are close to zero in the vicinity of the top of the interaction barrier near contact and which, later on, also tend to be dominated by the one-body dissipation, ref. 8) we have

$$\frac{d}{dt}(M_r U_z) = -\frac{1}{4}\rho\bar{v}\cdot a(t)\cdot 2U_z \quad , \tag{5}$$

where ρ is the mass density of nucleons (neutrons and protons) and M_r is the reduced mass, equal to $A_r m$, where $A_r = A_1A_2/(A_1 + A_2)$. Using eq. (5) to change the variable of integration in eq. (4) from t to U_z we find that the unknown window-area function a(t) cancels out. Using eq. (3) we then find

$$\Delta N_1 = (m/\rho\bar{v})\, 2A_r \int_c^{\nu_o} \frac{d\nu_z}{\nu_z} F_1(\nu_z)$$

$$= (N/A)\, 2A_r \int_c^{\nu_o} \frac{dx}{x}(x-c)^2\left[(1+c) - \frac{1}{3}c(x-c) - \frac{1}{12}(x-c)^2\right]$$

$$= \frac{1}{2}(N/A)\, A_r \left[\Phi(\eta,\nu_o) - \Phi(\eta,c)\right] \tag{6}$$

where

$$\Phi(\eta,x) = (\eta^2-1)^2 \ln x - \frac{8}{3}(\eta^3-1)x + (\eta^2+1)x^2 - \frac{1}{12}x^4 \quad , \tag{7}$$

ν_o is the initial radial velocity, U_o, in units of v_F, i.e.

$$\nu_o = U_o/v_F \tag{8}$$

and c stands for η - 1, the threshold value of ν_o.

The remarkable feature of eq. (6) is that its derivation did not require the solution of the time evolution of the collision dynamics. In particular, the knowledge of the form of the window-area function a(t) or of the radial velocity

function ν_z (t) was not needed. The final result is also independent, apart from the dimensionless escape velocity η, of any nuclear parameters. Even the quantity $\rho\overline{v}$, characteristic of the one-body dissipation dynamics, has canceled out. (In ref. 10 where the formula for Φ, eq. (7), was given, there is a misprint. In the second term in eq. (29) of ref. 10, p. 217, $1 - \eta^2$ should be replaced by $1 - \eta^3$.)

The total number of neutrons, ΔN, jetted through both nuclei A_1 and A_2 will be twice ΔN_1.

In the case of protons, the total number of particles jetted through both nuclei, ΔZ, will be the sum of two contributions similar to eq. (6), each with its characteristic escape velocity: η_1 for jetting through fragment A_1 and η_2 for jetting through fragment A_2. Thus

$$\Delta Z = (Z/A)\, A_r\, \frac{1}{2}\left[\Phi(\eta_1,\nu_o) + \Phi(\eta_2,\nu_o) - \Phi(\eta_1,c_1) - \Phi(\eta_2,c_2)\right] , \tag{9}$$

where $c_1 = \eta_1 - 1$ and $c_2 = \eta_2 - 1$.

In estimating the proton Coulomb barriers B_i in eq. (1) we shall keep in mind that the escaping proton is subjected to the electric field of the two nuclei in contact (and not just of the receptor nucleus). We shall accordingly write for B_i the estimate

$$B_i \approx \frac{Z_i e^2}{R_i} + \frac{(Z - Z_i - 1)e^2}{R_i + r_c} \approx \frac{(Z-1)e^2}{D_i} , \tag{10}$$

where r_c is the center separation at contact and D_i is the distance from the center of mass to the tip of the nucleus in question. Thus B_i is the Coulomb barrier at the tip of the receptor nucleus A_i. Since the jetting turns out to be focused around the line connecting the fragment centers, the neglect of the angular variation of the Coulomb barrier should not be serious. On the other hand, since the electric potential *inside* the colliding nuclei has been assumed constant, neither this estimate of B_i (nor that used in ref. (2)) is, strictly speaking, consistent with that assumption. As a result, we feel that the current estimates of ***proton*** jetting suffer from the further uncertainty of an inadequate

description of the electric forces, and should be treated with due reservations.

Consider now a collision at a finite impact parameter and finite angular momentum L. Let U_o denote, as before, the initial collision velocity at contact (when t = 0), and let $U_z(o)$ and $U_y(o)$ be the initial radial and tangential velocities, related to U_o and L by

$$U_o^2 = U_z^2(o) + U_y^2(o) \quad , \tag{11}$$

$$L = U_y(o) M_r r_c \quad . \tag{12}$$

If the effect of the centrifugal force on the equation of motion, eq. (5), is disregarded (see section 3e), the number of neutrons jetted at a given angular momentum L, say $\Delta N_1(L)$, will still be given by eq. (6), but with ν_o replaced by $\nu(o)$, where $\nu(o) \equiv U_z(o)/v_F$. (This is because the tangential component U_y does not influence the flux of jetted particles.) The average number of neutrons jetted through ***both*** fragments in a collision ranging over angular momenta from 0 to L will then be

$$\overline{\Delta N} = \int_o^L dL\, L\, \Delta N(L) \Big/ \int_o^L dL\, L \quad . \tag{13}$$

Since $dL^2 \propto dU_y^2(o) = -dU_z^2(o)$ in virtue of eqs. (11), (12), it follows that the number of jetted neutrons will be

$$\overline{\Delta N} = (N/A) \int_{\nu_L}^{\nu_o} dx\, x\, A_r \left[\Phi(\eta,x) - \Phi(\eta,c)\right] \Big/ \int_{\nu_L}^{\nu_o} dx\, x \tag{14}$$

$$= (N/A)\, A_r \left[\Psi(\eta,\nu_o) - \Psi(\eta,\nu_L)\right] \Big/ (\nu_o^2 - \nu_L^2) \quad , \tag{15}$$

where

$$\Psi(\eta,x) = (\eta^2-1)^2 x^2 \ln \frac{x}{\eta - 1} + \frac{1}{4}(\eta-1)^2(5 + 6\eta + 5\eta^2)x^2$$

$$- \frac{16}{9}(\eta^3 - 1)x^3 + \frac{1}{2}(\eta^2 + 1)x^4 - \frac{1}{36}x^6 \quad . \tag{16}$$

Here ν_L is the radial velocity (in units of v_F) at the impact parameter corresponding to the highest angular momentum, L. Thus

$$\nu_L^2 = \nu_o^2 - (L/M_r\, r_c\, v_F)^2 \quad . \tag{17}$$

The number of jetted protons will be

$$\overline{\Delta Z} = (Z/A)\, A_r\, \frac{1}{2} \left[\Psi(\eta_1,\nu_o) + \Psi(\eta_2,\nu_o) - \Psi(\eta_1,\nu_L) - \Psi(\eta_2,\nu_L)\right] \Big/ (\nu_o^2 - \nu_L^2) \quad . \tag{18}$$

The actual value of the upper limit L (or the lower limit ν_L) will depend on the type of process under consideration. If the experimental measurement of the jetting is associated with the detection of all types of reactions initiated by any impact parameter, then ν_L will be equal to c, (c_1 or c_2 in the case of protons) the critical radial velocity below which jetting does not occur. If the measurement is confined to evaporation-residue products (so that fission reactions are not registered) then, for the heavier systems, a relatively lower limiting value on L (a higher limit on ν_L) will be imposed by the requirement that the rotating compound nucleus should survive fission during the de-excitation stage. The condition for survival is, approximately, that the fission barrier should exceed the neutron binding energy. If the nucleus is idealized as a rotating liquid drop, then the cut-off angular momentum is given by

$$L = \left(\frac{4}{5} r_o^2 m a_2 A^{\frac{7}{3}} y_s\right)^{\frac{1}{2}} \quad , \tag{19}$$

where r_o^2 is the nucleon radius constant (1.22 fm), m the nucleon mass (mc^2 = 938 MeV), a_2 is the surface energy coefficient (17.62 MeV), and y_s is the value of the dimensionless rotational parameter of ref. (11) at which the fission barrier of the rotating nucleus has been reduced to S MeV, a typical nucleon binding energy of 8–10 MeV in the present context.

The cross section for neutron jetting through nucleus A_1 is obtained by multiplying $\overline{\Delta N_1}$ by the area of the impact-parameter circle, πb^2, where b is the impact parameter associated with the highest contributing angular momentum L. Thus

$$\sigma_{tot} = \pi b^2\, \overline{\Delta N_1} \quad , \tag{20}$$

where

$$b = L/M_r U_\infty \quad . \tag{21}$$

d) *The Velocity Anomaly in Head-on Collisions*

Let the velocity of the projectile in the laboratory frame during a head-on collision be $U_P(t)$ and of the target $U_T(t)$, so that

$$U(t) = U_P(t) - U_T(t) \tag{22}$$

is the relative (radial) velocity. The number of neutrons jetted in time dt is $F_n(t)\, a(t)dt$ and, insofar as the jetting is inversion symmetric in the instantaneous mid-velocity frame, the momentum carried away by the jetted neutrons is simply

$$F_n(t)\, a(t)\, \frac{1}{2}(U_P + U_T)\, m\, dt \quad . \tag{23}$$

Let us write the number of protons jetted in time dt as $F_p(t)\, a(t)\, dt$ and the total number of particles jetted in time dt as $F(t)\, a(t)\, dt$, where $F = F_n + F_p$. The proton jetting is inhibited to a certain extent by the Coulomb barrier, which increases the escape velocities η_1, η_2 above the value η for neutrons. In what follows we shall estimate the momentum carried away by neutrons and protons by multiplying eq. (23) by (A/N) and by using an effective value of η somewhat higher than would be appropriate for neutrons alone. Since, for protons, the inversion symmetry of jetting is broken to the extent that $\eta_1 \neq \eta_2$, the equations that follow are only approximate to the extent that the (minor) proton component of the jetting is not treated accurately. With this approximation, the total momentum carried away during the jetting is

$$\Delta P = (A/N) \int_0^{t_c} \tfrac{1}{2}(U_P + U_T)\, m F_n\, a\, dt \quad . \tag{24}$$

Using eq. (22) and the momentum conservation equation

$$A_P U_P + A_T U_T = A_P U_\infty \quad , \tag{25}$$

where U_∞ is the initial projectile velocity in the laboratory frame, we have

$$U_T = (U_\infty - U)A_P/A \tag{26}$$

$$U_P = (U_\infty A_P + UA_T)/A \quad , \tag{27}$$

so that

$$\Delta P = (A/N)\int_o^{t_c} 1/2\left[\frac{2A_P}{A}U_\infty + \frac{A_T - A_P}{A}U\right] m\, F_n\, a\, dt \quad . \tag{28}$$

Again using eq. (5) to replace dt by dU we find

$$\Delta P = \frac{A_P}{A} m U_\infty\, \Delta A + \frac{A_T - A_P}{A} A_r m \int_{U_c}^{U_o} \frac{F_n}{\rho_n \bar{v}/m}\, d\,U \quad , \tag{29}$$

where $U_c = cv_F$, U_o is the relative velocity at contact and ΔA is the total number of jetted particles.

The momentum of the compound nucleus after jetting is $mA_PU_\infty - \Delta P$, and its velocity is $(mA_PU_\infty - \Delta P)/m(A - \Delta A)$. We shall define the relative velocity anomaly, $\Delta v/v_{ref}$, as the difference between what the velocity would be in the absence of jetting (i.e., the reference velocity, $v_{ref} = A_PU_\infty/A$) and the actual velocity, divided by v_{ref}. Assuming that $\Delta A \ll A$, we find

$$\frac{\Delta v}{v_{ref}} = \frac{A_T(A_T - A_P)}{A^2U_\infty}\int_{U_c}^{U_o} \frac{F_n(U)}{\rho_n \bar{v}/m}\, dU$$

$$= \frac{2A_T(A_T - A_P)}{A^2\nu_\infty}\int_c^{\nu_o} dx(x-c)^2\left[(1+c) - \frac{1}{3}c(x-c) - \frac{1}{12}(x-c)^2\right]$$

$$= \frac{A_T(A_T - A_P)}{A^2\nu_\infty}\left[\frac{2}{3}(\nu_o - c)^3 - \frac{1}{6}(\nu_o - c)^4 - \frac{1}{30}(\nu_o - c)^5\right] , \tag{30}$$

where $\nu_\infty = U_\infty/v_F$. The discussion of the time-development of the collision dynamics has been once again by-passed in the derivation of eq. (30).

e) *Improved Treatment of Jetting in Collisions at Finite Impact Parameters*

For a given collision energy, the radial velocity at contact decreases with increasing impact parameter (according to eq. (11). Since jetting is a steep function of the excess of the radial velocity over the threshold value, most of the jetting will be due to collisions with small impact parameters, for which the closed formulae given in the previous sections will continue to be fair approximations. Improved formulae for some aspects of jetting involving finite impact parameters can be derived under certain assumptions.

For a non-central collision the equations of motion for the radial and tangential components U_z and U_y are the coupled equations

$$\frac{d}{dt}(M_r U_z) = -\tfrac{1}{2}\rho\bar{v}aU_z - \frac{M_r U_y^2}{r} + \frac{\partial V}{\partial r} \quad , \tag{31}$$

$$\frac{d}{dt}(M_r U_y r) = -\frac{1}{4}\rho\bar{v}aU_y r \quad , \tag{32}$$

where r is the distance between the mass centers of the nuclei and $\partial V/\partial r$ is the conservative force, disregarded in what follows (see sec. 3c). In eq. (31) the rate of change of radial momentum is equated to the sum of frictional, centrifugal and conservative forces. In eq. (32) the rate of change of orbital angular momentum is equated to the torque due to the presence of the tangential window friction. (The torque on fragment A_1 is $\frac{1}{4}\rho\bar{v}aU_y r_1$, the torque on A_2 is $\frac{1}{4}\rho\bar{v}aU_y r_2$ and these are the rates of change of the angular momentum of A_1 and A_2. The sum of the torques, $\frac{1}{4}\rho\bar{v}aU_y r$, is then the negative of the rate of change of the orbital angular momentum. Here r_1 and r_2 are the distances of the window from the centers of A_1 and A_2, respectively.)

Since the inward radial velocity U_z is given by $-(dr/dt)$ we may rewrite eqs. (31), (32) as follows:

$$\frac{dU_z}{dt} = -(\rho\bar{v}a/2M_r)\,U_z - \frac{U_y^2}{r} \quad . \tag{33}$$

$$\frac{dU_y}{dt} = -(\rho\bar{v}a/4M_r)\,U_y + \frac{U_yU_z}{r} \quad . \tag{34}$$

We shall now argue that the last two terms in both these equations are formally small and can be disregarded for collision velocities small compared to $\bar{v}$. We first estimate the order of magnitude of the stopping distance Δr in which the radial velocity U_z is brought to zero. Except when the centrifugal term U_y^2/r dominates, the equation for U_z may be replaced, for the purpose of an order of magnitude estimate, by

$$\frac{dU_z}{dt} \approx -(\rho\bar{v}\,\bar{a}/2M_r)\,U_z \quad , \tag{35}$$

where $\bar{a}$ is some representative window area. For such motion the stopping distance is of order

$$\Delta r \approx 2M_rU_z(o)/\rho\bar{v}\,\bar{a} \quad , \tag{36}$$

where $U_z(o)$ is the initial value of U_z. Now for two spheres with radii R_1, R_2, which overlap by a distance Δr, the radius r_w of the window defined by their intersection is (by elementary geometry)

$$r_w \approx \sqrt{2\bar{R}\Delta r} \quad , \tag{37}$$

Where $\bar{R}$ is the reduced radius of the system, equal to $R_1R_2/(R_1 + R_2)$. Combining eqs.(36) and (37) we find for the representative value of the window area $\bar{a}$ in a collision with initial radial velocity $U_z(o)$, the order of magnitude relation.

$$\bar{a} \approx (4\pi\bar{R}M_rU_z(o)/\rho\bar{v})^{1/2} \quad . \tag{38}$$

Using this estimate of $\bar{a}$, a representative value of the ratio of the centrifugal term U_y^2/r to the frictional term in eq. (33) is

$$\left(\frac{U_y}{U_z}\right)\left(\frac{U_y}{\bar{v}}\right)\left(\frac{\bar{v}M_r}{\pi\bar{R}r^2\rho U_z(o)}\right)^{1/2} \quad .$$

In order of magnitude, $\pi\bar{R}r^2\rho$ cancels against M_r, and we find for the above ratio the order of magnitude estimate

$$\left(\frac{U_y}{U_z}\right)^{3/2} \left(\frac{U_y}{\bar{v}}\right)^{1/2} .$$

Since U_y is small compared to $\bar{v}$ and, for situations relevant for jetting, U_y is also small compared to U_z, the neglect of the centrifugal term in eq. (33) is formally justified.

A similar estimate applied to eq. (34) gives for the ratio of the term $U_y U_z/r$ to the frictional term the order of magnitude estimate $(U_z/\bar{v})^{1/2}$. This is still formally a small quantity when U_z is small compared to $\bar{v}$.

Neglecting the last terms in both eqs. (33) and (34), we arrive at the simplifying estimate

$$\frac{1}{U_z}\frac{dU_z}{dt} \approx \frac{2}{U_y}\frac{dU_y}{dt} . \tag{39}$$

This leads to the relation

$$\frac{U_y}{U_y(o)} \approx \left(\frac{U_z}{U_z(o)}\right)^{1/2} , \tag{40}$$

which makes possible further progress in the derivation of closed formulae for jetting properties.

f) *The Velocity Anomaly for Arbitrary Collisions*

We repeat the analysis of sec. 3d, focusing attention on velocity components parallel to the (original) beam direction, denoted by a subscript ||. These are the only components that influence the velocity anomaly. We again neglect the breaking of inversion symmetry in the case of proton jetting. Moreover, we found by numerical tests that, for collision velocities relevant for jetting, the Coulomb deflections of the colliding nuclei may be neglected for the purposes of a rough estimate. With these assumptions, the momentum carried away by the jetted particles is found to be given by the generalization of eq. (28):

$$\Delta P = (A/N)\int_o^{t_c} \tfrac{1}{2}\left(\frac{2A_P}{A} U_\infty + \frac{A_T - A_P}{A} U_{||}\right) m F_n \, a \, dt. \tag{41}$$

Here $U_{\|}$ is the component parallel to the beam direction of the instantaneous relative velocity $\vec{U}$. Since $\vec{U}$ has components U_z and U_y and since the beam direction has been assumed to coincide with the initial relative velocity at contact, whose components are $U_z(o)$ and $U_y(o)$, $U_{\|}$ is found by taking the scalar product of the vector (U_z, U_y) with the unit vector $(U_z(o), U_y(o))/U_o$, i.e.,

$$U_{\|} = \left[U_z(o)U_z + U_y(o)U_y\right]\Big/U_o$$

$$= \left[U_z(o)U_z + U_y^2(o)\left(U_z/U_z(o)\right)^{1/2}\right]\Big/U_o$$

$$= \left[U_z(o)U_z + \left(U_o^2 - U_z^2(o)\right)\left(U_z/U_z(o)\right)^{1/2}\right]\Big/U_o \quad . \tag{42}$$

Changing the variable of integration from t to U_z, as before, and averaging over angular momenta from 0 to L, as in sec. 3c, we find the following expression for the average velocity anomaly:

$$\frac{\Delta v}{v_{ref}} = \frac{2A_T(A_T - A_P)}{A^2\nu_\infty\nu_o(\nu_o^2 - \nu_L^2)}\left[\chi(\nu_o) - \chi(\nu_L)\right] , \tag{43}$$

where

$$\chi(x) = -c_1x^3 - c_2x^4 + c_3x^5 - c_4x^6 + (x^8/4320)$$

$$+ \nu_o^2\left[4c_2x^2 - \frac{20}{3}c_3x^3 + 9c_4x^4 - (x^6/324)\right] - c_5\left[\frac{2}{3}\nu_0^2x^{3/2} - \frac{2}{7}x^{7/2}\right] , \tag{44}$$

with

$$c_1 = c^3(1 + c + \frac{1}{5}c^2)/9$$

$$c_2 = c^2(1 + c + \frac{1}{4}c^2)/4$$

$$c_3 = c(1 + c + \frac{1}{3}c^2)/15$$

$$c_4 = (1 + c + \frac{1}{2}c^2)/90$$

$$c_5 = 16c^{5/2}(1 + c + \frac{2}{9}c^2)/15. \tag{45}$$

The definitions of ν_o, ν_∞ are as in sec. 3d and ν_L is given by eq. (17).

Figs. 3a, 3b show the result of applying the equations of this section to a number of reactions studied experimentally. The data are taken from ref. 9, due mainly to experiments at the 88" cyclotron in Berkeley and the VICKSI accelerator of the Hahn-Meitner Institute in Berlin. The data refer to the velocities of evaporation residues, i.e., to fusion products that survived fission. Accordingly, the value of the cut-off angular momentum L specifying ν_L in eq. (43) was taken to be that angular momentum beyond which fission would be expected to dominate over nucleon evaporation, i.e., we used eq. (19). We took 10 MeV as a representative value of the average separation energy for neutrons and protons.

Fig. 3a shows how the total number of jetted particles increases rapidly with the collision velocity. Note that the "universal" curve for head-on collisions (independent of the masses of the collision partners) is a rough guide to the properly L-averaged results (circled points). Fig. 3b compares the calculated relative velocity anomaly $\Delta v/v_{ref}$ with measurements. It would appear that Fermi jetting can make only a modest contribution to the observed velocity anomaly. It is, in fact, likely that most of the anomaly is due to a different mechanism involving peripheral collisions (Ref. 12).

4. *Numerical Calculation of Differential Cross Sections*

Refering to Fig. 1 and section 3, a jetting event initiated by a given collision velocity U_o is a function of the three components of the Fermi-gas velocity $\vec{v}$, of the angular momentum and of the time. The angular momentum may be specified by $U_y(o)$ and, as we saw, the time interval dt is proportional to dU_z/U_z. Thus the final vector velocity of the jetted particle (denoted by $\vec{w}'$ in the target reference frame and by $\vec{u}$ in the center of mass frame) can be written as a function of the parameter U_o and of the five variables v_x, v_y, v_z, $U_y(o)$, U_z, i.e.,

$$\vec{u}(U_o; v_x, v_y, v_z, U_y(o), U_z) \quad . \tag{46}$$

Each choice of the five variables will lead to a jetting velocity representable by a point in the three-dimensional velocity space of $\vec{u}$. In the numerical calculation,

the five-dimensional space of the variables v_x,....U_z was covered by a suitable grid and the initial conditions defined by this grid were mapped into the space of $\vec{u}$ by following the refraction of the trajectory at the exit point X in Fig. 1 and by performing the center-of-mass transformation. The points thus accumulated in the $\vec{u}$ space were collected within given ranges of the velocity u or the energy $mu^2/2$, and of the angle of $\vec{u}$ with the beam axis. In this way histograms of the angular and energy (or velocity) distributions were constructed numerically.

In the case of proton jetting, the deflection of the outgoing proton in the field of the fusing system was estimated by using the monopole component of this field, i.e., by calculating the deflection caused by the residual charge $(Z - 1)e$ placed at the center of mass.

Once the problem of jetting is treated numerically, one may attempt to study the effect of absorption of the jetted nucleons when traversing the receptor nuclei. In practice it is not clear how to do this in a realistic way. An extreme assumption is to take an absorption mean free path λ, estimated from the imaginary part of the nuclear optical potential, and to reduce the number of jetted particles by a factor $\exp(-d/\lambda)$, where d is the distance traversed by the particle inside the receptor nucleus. This is likely to be an overestimate of the effect of absorption, since λ represents the mean free path for taking a particle out of the elastic scattering channel whereas, from the point of view of jetting, particles taken out of the elastic channel can still in many cases escape, albeit with a reduced energy and at a modified jetting angle. (These are the "two-body" PEPs of ref. (2).) Furthermore, the probability for absorbing a nucleon traversing a nucleus is most likely greater in the surface region than in the bulk. Since, in a scattering experiment, a nucleon traverses in general the surface region twice, but in a jetting process only once, the use of the mean free path λ deduced from the optical potential may not be appropriate for jetting. (We may note here that bulk absorption breaks the inversion symmetry for jetting in the case of unequal nuclei, but pure surface absorption would leave it intact.)

Keeping all these uncertainties and reservations in mind we will nevertheless present, for orientation, results in which the factor $\exp(-d/\lambda)$ was included, with λ given by

$$\lambda = \frac{\hbar w}{V_{imag}} \quad , \tag{47}$$

where the imaginary potential V_{imag} was parameterized to represent approximately Fig. 2-29 of ref. (13), i.e.,

$$V_{imag} = 3\ \text{MeV} + 0.07E_F(w'/v_F)^2 \quad . \tag{48}$$

Here w is the nucleon velocity inside and w' is the velocity outside the receptor nucleus.

We found that, in agreement with ref. 4, this treatment of absorption reduces considerably the absolute values of the jetting cross-sections, while changing the shapes of the energy and angular spectra relatively little. In view of what was said above, this treatment of absorption probably overestimates the suppression of the Fermi jets.

5. *Comparison with Other Jetting Calculations*

We are now in a position to compare some of our results with earlier calculations in refs. (2), (4). The first example is neutron jetting in the reaction $^{12}C + {}^{158}Gd$ at $E_{LAB} = 152$ MeV, considered in ref. (2). The energy spectra are shown in Fig. 4a and the angular distributions for neutrons with center-of-mass energies greater than 14 MeV are shown in Fig. 4b. We used a collision velocity $U_{\delta} = 0.524v_F$, obtained by estimating the Coulomb barrier between ^{12}C and ^{158}Gd according to the proximity potential of ref. (14). For the angular momentum cut-off L we used the fusion condition which, for this light system, effectively puts ν_L equal to c. The smooth curves in Fig. 4a are based on histograms with a step size of 1 MeV.

The results of ref.(2) contain both "one-body" jets, corresponding to the present treatment, as well as "two-body" jets. The latter result from processes

where a jetting nucleon collides with another nucleon before escaping. With our schematic treatment of absorption, such nucleons do not contribute to our cross sections. The authors of ref. (2) state that two-body jets contribute 30% to the total jetting cross section. With a reported cross section of 600 mb, the one-body contribution would be about 460 mb, in reasonable agreement with our calculation, which corresponds to 470 mb.

Owing, presumably, to the different approximations made, our jetting spectra are centered at somewhat lower energies and are slightly more focused in the forward direction. In fact, for the high-energy neutrons above 14 MeV, our results are lower by a factor of about 2, as shown in Fig. 4b.

As regards the proton cross sections, the differences between our results and those of ref. (2) are more pronounced. As mentioned in sec. 3c, both results on proton jetting should, we feel, be taken with reservations.

In Fig. 5 we compare our calculations with those of ref. (4) for the reaction $^{16}O + ^{93}Nb$ at $E_{LAB} = 204$ MeV. In ref. (4) no distinction is made between protons and neutrons, i.e., Coulomb effects are ignored. Similarly, in order to make our results comparable, we made our calculations for neutrons and multiplied the resulting numbers by A/N. We used in this calculation the value $E_F = 37.8$ MeV (as in ref. (4)) and we compare cross sections for the case of no absorption to the corresponding results of ref. (4).

Fig. 5 shows that the forms of the energy and angular distributions are similar in the two calculations, but there is a discrepancy of about a factor of 2.3 in absolute magnitudes. (A total cross section of 1083 mb compared to 463 mb.) This may be due to the different collision dynamics used in the two calculations. In ref.(4) a considerably "harder" friction is used, which slows down the nuclei at a relatively larger separation, when the window area is smaller. It is believed (ref. (15)) that, by varying the friction form factor, the total cross section could be changed by a factor of 2 or so. This confirms the expectation, mentioned in the introduction, that Fermi jets might provide a sensitive test of the friction

form factor.

Although the above comparisons are far from exhaustive and cannot be made unambiguous due to the different assumptions and approximations, there is a qualitative correspondence in the results and the quantitative differences may well be within the expected range.

6. *Cross Sections: Gaussian Parameterization and Systematics*

In this section we shall use our model to discuss the properties of Fermi jets in a more systematic way for a wide range of heavy ion reactions.

For an economic way of doing this, the following observation is most helpful. It turns out that in all cases we considered, the angular-momentum-averaged center-of-mass distribution of the neutrons jetted through one of the fragments resembles to a good approximation a Gaussian in velocity space. Thus, the triple differential cross section in the velocity space $\vec{u}$, for jetting neutrons through nucleus A_1, may be written as

$$\frac{d^3\sigma}{d^3u} = \frac{d^3\sigma}{du_\parallel du_\perp u_\perp d\phi} \approx \frac{\sigma_{tot}}{\pi^{3/2}\Delta_\perp \Delta_\parallel^{1/2}} \exp\left\{-\frac{(u_\parallel - \overline{u_\parallel})^2}{\Delta_\parallel} - \frac{u_\perp^2}{\Delta_\perp}\right\} , \tag{49}$$

where $u_\parallel$, $u_\perp$ and ϕ are cylindrical polar coordinates of $\vec{u}$, with $u_\parallel$ along and $u_\perp$ perpendicular to the beam, so that $du_\parallel du_\perp u_\perp d\phi$ is the volume element in velocity space. (The ϕ used in this equation is not to be confused with the ϕ in Fig. 1). Eq. (49) implies that the distribution of the jetted neutrons may be specified by four parameters: σ_{tot}, $\overline{u_\parallel}$, $\Delta_\parallel$ and $\Delta_\perp$. These may be expressed in terms of four moment integrals as follows:

$$\sigma_{tot} = \pi b^2 \overline{\Delta N_1} \ , \tag{50}$$

$$\Delta_\parallel = 2(\overline{u_\parallel^2} - \overline{u_\parallel}^2) \tag{51}$$

$$\Delta_\perp = \overline{u_\perp^2} \ , \tag{52}$$

where

$$\overline{\Delta N_1} = \int 1 \qquad \textbf{(53)}$$

$$\overline{u_\parallel} = \int u_\parallel \Big/ \overline{\Delta N_1} \qquad (54)$$

$$\overline{u_\parallel^2} = \int u_\parallel^2 \Big/ \overline{\Delta N_1} \qquad (55)$$

$$\overline{u_\perp^2} = \int u_\perp^2 \Big/ \overline{\Delta N_1} \ . \qquad (56)$$

In the above, $\int (...)$ stands for the following five-fold integral:

$$\int (...) = \frac{(4NA_T / \pi A v_F^4)}{U_o^2 - U_L^2} \int_{U_L}^{U_o} dU_z(o) U_z(o) \int_o^{U_z(o)} \frac{dU_z}{U_z} \cdot$$

$$\cdot \int_{w_e - U_z}^{v_F} dv_z (v_z + U_z) \int_o^{\sqrt{v_F^2 - v_z^2}} dv_t v_t \int_o^{2\pi} d\psi e^{-d/\lambda} (...) \ , \qquad (57)$$

where $v_t = \sqrt{v_x^2 + v_y^2}$. The integral for $\overline{\Delta N_1}$ merely restates the integrations involved in evaluating, in section 3c, the number of neutrons jetted through nucleus A_1 (with the absorption factor included) and the other integrals are the moments required in evaluating the parameters of the Gaussian. We carried out the integrations numerically.

Transforming from velocity space to energy-angle space E, θ in the center of mass, we find the following expression for the differential cross section

$$\frac{d\sigma}{dE d\Omega} = (\sigma_{tot}/m)\, (\pi^{3/2}\, \Delta_\perp\, \Delta_\parallel^{1/2})^{-1}\, (2E/m)^{1/2} \cdot$$

$$\exp \left\{ - (2E/m\Delta_\parallel) \cos^2\theta - (2E/m\Delta_\perp) \sin^2\theta - \overline{u_\parallel}^2/\Delta_\parallel + (2\overline{u_\parallel}/\Delta_\parallel)\, (2E/m)^{1/2} \cos\theta \right\} . \qquad \ldots . (58)$$

A parameterization similar to eq. (49) was found useful for *protons* jetted through nucleus A_1. However, we have to take into account the acceleration of the protons in the field of the fusing nucleus. The main effect of this acceleration is a boost in energy approximately equal to the height of the Coulomb barrier at the tip of the receptor nucleus. Thus, a fair approximation to the proton

distribution in velocity space turned out to be the following distorted Gaussian

$$\frac{d^3\sigma}{d^3u} = \frac{\Gamma\sigma_{tot}}{\pi^{3/2}\Delta_\perp\sqrt{\Delta_\parallel}} \exp\left\{-\frac{(\Gamma u_\parallel - \overline{u_\parallel})^2}{\Delta_\parallel} - \frac{(\Gamma u_\perp)^2}{\Delta_\perp}\right\}, \tag{59}$$

where

$$\Gamma = 1 - \frac{B_1}{\frac{m}{2}(u_\parallel^2 + u_\perp^2)} \tag{60}$$

and the energy shift B_1 is given by eq. (10).

The expressions for the parameters σ_{tot}, $\overline{u_\parallel}$, $\Delta_\parallel$ and $\Delta_\perp$ etc., resemble equations (50)-(56), but with $u_\parallel$ and $u_\perp$ replaced by $\Gamma u_\parallel$ and $\Gamma u_\perp$ in the integrands. Similarly, the energy-angle distribution resembles eq. (58), but with E replaced by $E-B_1$ on the right hand side.

Fig. 6 gives an example of the quality of the parameterization of the energy and angular spectra by means of the Gaussian functions, for neutrons as well as protons. With the differential cross-sections expressible approximately in terms of four parameters, it is now possible to give a broad survey of the results for virtually any combination of target and projectile and for all bombarding energies of interest. We shall present the results concerning σ_{tot}, $\overline{u_\parallel}$, $\Delta_\parallel$ and $\Delta_\perp$ as functions of three parameters: the total mass number $A = A_1 + A_2$, the asymmetry α defined by

$$\alpha = \frac{A_1 - A_2}{A_1 + A_2}, \tag{61}$$

and the center-of-mass collision velocity at contact, U_o. The atomic numbers Z_1, Z_2 are not considered as independent parameters, but are assumed to correspond to the location of Green's valley of beta stability for each nucleus, viz.

$$Z_i = \tfrac{1}{2}A_i\left(1 - \frac{0.4A_i}{200 + A_i}\right). \tag{62}$$

We focus attention on jetting associated with fusion followed by de-excitation by particle emission rather than fission. This means that we use for the cut-off angular momentum the procedure described in sec. 3c, so that for heavier systems L is determined by eq. (19). (This time we took S = 8 MeV as a typical nucleon separation energy and added the Coulomb barrier for protons according to eq. (10).) For the nuclei defined by eq. (62) and for A between 40 and 240, the rotational parameter y_8, where the fission barrier is reduced to 8 MeV, can be approximated by

$$y_8 \approx 0.1195\, X^2 - 0.0215\, X^3 \quad , \tag{63}$$

$$\text{where } X = (A - 250) / 100 \quad . \tag{64}$$

Figs. 7–11 display the calculated values of $\sigma_{tot}\overline{u_\parallel}$, $\Delta_\parallel$ and $\Delta_\perp$ for both neutron and protron jets as functions of α for various values of A and U_o. For a positive α, the resuls refer to jetting through nucleus A_1. Jetting through nucleus A_2 corresponds to negative α. In most experimental situations the larger nucleus would be the target, so in such cases positive values of α correspond to jetting through the target (forward jets) and negative values of α to (backward) jetting through the projectile.

Fig. 7 shows total cross-sections for jetting in the absence of absorption. Owing to the inversion symmetry for jetting, the curves for neutron jetting are symmetric about $\alpha = 0$. Proton jetting through the lighter nucleus ($\alpha < 0$) is favored because of the lower Coulomb barrier implied by eq. (10). The cross sections rise steeply with the collision velocity U_o. As a function of A they go through a maximum around $A \approx 120$. The effect of including absorption is shown in Fig. 8. The cross sections are reduced by a factor of 2–4 (probably an overestimate) and an asymmetry with respect to α is introduced for neutrons as well as protons, the absorption being greater for jetting through the larger nucleus. (This would not be the case for surface rather than volume absorption.) The shapes of the differential cross sections, as opposed to their absolute magni-

tudes, turned out to be very insensitive to the absorption as included here. Thus the values of $\overline{u_\parallel}$, $\Delta_\parallel$ and $\Delta_\perp$ changed only at the percent level and in what follows we shall only display the results for no absorption.

Fig. 9 shows the values of $\overline{u_\parallel}$. In the case of neutrons, in particular, one can see clearly the two limiting situations in which the L cut-off is dictated either by the threshold value U_c (dot-dashed curve) or by the onset of fission (dashed-curve). In the case of protons, the escape velocity and, consequently, U_c, depends on the colliding nuclei and the limiting behaviors do not stand out so clearly.

Since $\overline{u_\parallel}$ reflects the average velocity parallel to the beam in the center of mass, it is strongly asymmetric with respect to $\alpha = 0$, the asymmetry rising with increasing U_o.

The values of the widths $\Delta_\parallel$ and $\Delta_\perp$ are displayed in Figs. 10 and 11. As seen from the trends of $\Delta_\perp$, jets are optimally focused for nearly symmetric collisions. This, together with the existence of a maximum in the total cross sections for A~120, suggests that collisions of two approximately equal nuclei with mass numbers around 60 might provide certain advantages for the observation of Fermi jets. We took the case A = 120, $\alpha = 0$ to display in greater detail the U_o-dependence of the Gaussian parameters for both neutrons and protons. (The implied units of $\overline{u_\parallel}$ are v_F and of $\Delta_\parallel$ and of $\Delta_\perp$ are v_F^2. The units of σ_{tot} are millibarns.) All quantities refer to calculations without absorption.

We note the rapid rise of the cross sections with increase of U_o over the threshold value U_c. The slowing down of the rise around $U_o \approx (0.5-0.6)v_F$ is a hint of the eventual saturation of the cross sections that would take place when all the available nucleons have acquired velocities exceeding the escape velocity. Long before this has happened, the approximations of our treatment become unrealistic and this saturation-like trend of the cross section curves is a reminder that none of the results should be taken at face value when the collision velocity is no longer small compared to the Fermi velocity v_F or, equivalently,

when the number of jetted particles is no longer small compared to the number of available nucleons. An interesting feature of Fig. 12 is the tendency for the transverse width $\Delta_\perp$ to saturate near $U_o \approx 0.4 v_F$ and even to decrease later. Thus the focusing of the jets would be expected to be best for low and high collision velocities, which appears plausible on qualitative grounds.

7. *Summary and Conclusions*

As a step towards a better understanding of the prompt emission of nucleons in the early stages of a nucleus-nucleus collision, we have worked out in some detail an idealized model of Fermi jets. At the price of several simplifying assumptions, we have been able to provide a broad survey of the expected features of the jetted nucleons. The quantitative features of these results should be taken with considerable reservations. The most serious shortcomings of the present treatment are probably the use of geometrical optics in tracing the nucleon trajectories, the disregard of the diffuseness of the nuclear surface, the uncertainty in the treatment of absorption, and the schematic approximations concerning the electric forces acting on the protons. In particular, the use of classical trajectories instead of wave mechanics could be misleading in the case of nucleons with low emission velocities. Because of the uncertainty principle, particles possessing low angular momenta would in reality have much more nearly isotropic distributions than the classical calculations indicate. The uncertainties associated with absorption might affect mostly the absolute magnitudes rather than the intrinsic shapes of the differential cross sections. The treatment of proton jetting calls for obvious improvements.

With all these reservations in mind, we still hope that a sufficiently comprehensive comparison of suitable experimental data with the present idealized model (or a somewhat improved future version) may begin to reveal tell-tale correspondences. This could be followed by more incisive experiments and calculations, which would identify unambiguously the Fermi-jetting mechanism and, eventually, lead to an improvement in our understanding of the dynamics of

nucleus-nucleus collisions.

Acknowledgements

The authors are indebted to the Lawrence Berkeley Laboratory and to the Hahn-Meitner Institute for making this collaboration possible. Numerous helpful discussions with M. Blann, Yuen-Dat Chan, and R. Stokstad are gratefully acknowledged. K.M. and M.Z.-P. would like to thank the Lawrence Berkeley Laboratory's Nuclear Science Division for the hospitality extended to them during their stay in Berkeley.

This work was supported in part by the Director, Office of Energy Research, Division of Nuclear Physics of the Office of High Energy and Nuclear Physics of the U.S. Department of Energy under Contract DE-AC03-76SF00098.

References

[1] J. P. Bondorf, J. de Physique **C5** (1976) 195.

[2] J. P. Bondorf, J. N. De, G. Fai, and A. O. T. Karvinen, Nucl. Phys. **A333** (1980) 285.

[3] M. C. Robel, Ph.D. thesis, Lawrence Berkeley Laboratory preprint LBL-8181 (1979), unpublished.

[4] K. T. R. Davies, B. Remaud, M. Strayer, K. R. Sandya Devi, and Y. Raffray, Ann. of Phys. **156** (1984) 68.

[5] M. Blann and H.K. Vonach, Phys. Rev. **C28** (1983) 1475.

[6] For example, W.D. Myers and W.J. Swiatecki, Annals of Phys. **55** (1969) 395.

[7] D. H. E. Gross and H. Kalinowski, Phys. Rep. **45** (1978) 175.

[8] J. Blocki, Y. Boneh, J. R. Nix, J. Randrup, M. Robel, A. J. Sierk, and W. J. Swiatecki, Annals of Phys. **113** (1978) 330; see also ref. 10.

[9] Y. Chan, C. Albiston, M. Bantel, P. Countryman, D. DiGregorio, R. G. Stokstad, S. Wald, S. Zhou, Z. Zhou, A. Budzanowski, K. Grotowski and R. Planeta, "Velocity Distribution of Fusion-like Products for medium mass heavy-ion systems". Proc. of the Workshop on Nuclear Dynamics III, ed. V. Viola, 5–9 March 1984, Copper Mountain, Colorado, p. 131; Y. Chan, M. Murphy, R. G. Stokstad, I. Tserruya, S. Wald and A. Budzanowski, Phys. Rev. **C27** (1983) 447; Y. Chan, private communication, 1983.

[10] W. J. Swiatecki, "Macroscopic Treatment of Nuclear Dynamics", Lawrence Berkeley Laboratory preprint LBL-17837, May 1984 and Proc. Int. Conf. on Theoretical Approaches to Heavy Ion Reaction Mechanisms, Paris, May 14–18, 1984, Nucl. Phys. **A428** (1984) 199c.

[11] S. Cohen, F. Plasil, and W. J. Swiatecki, Annals of Phys. **82** (1974) 557.

[12] B. G. Harvey and H. Homeyer, Lawrence Berkeley Laboratory preprint LBL-16882 (1983).

[13] A. Bohr and B. Mottelson, "Nuclear Structure" Vol. I, W. A. Benjamin Inc., 1969.

[14] J. Blocki, J. Randrup, W. J. Swiatecki, and C. F. Tsang, Annals of Phys. **105** (1977) 427.

[15] B. Remaud, private communication, 1984.

Figure Captions

Fig. 1 The geometry of the jetting process. Two nuclei A_1 and A_2 are shown soon after contact, when a small window W has opened between them. The relative velocity of A_2 with respect to A_1 is $\vec{U}$, with component U_z along the line of centers and U_y in the tangent plane. This velocity is added to the Fermi-gas velocity $\vec{v}$ of a nucleon from A_2, to produce an injection velocity $\vec{w}$ of the nucleon entering A_1. The angles of $\vec{U}$ and $\vec{w}$ with the z-axis are denoted by α and β, and the azimuthal angle of $\vec{v}$ is denoted by ψ. The injected nucleon leaves nucleus A_1 at the exit point X with a refracted velocity $\vec{w}'$, related to $\vec{w}$ by an appropriate reduction of the component normal to the surface of A_1 at X. The jetting takes place in the plane WXF, inclined at an angle ϕ to the reaction plane. The line joining the center of mass, CM, to X makes an angle δ with the z-axis.

Fig. 2 The velocity space as seen from a coordinate system fixed in nucleus A_1. The location of the center of the Fermi sphere associated with nucleons in A_2 is given by the relative-velocity vector $\vec{U}$ lying in the plane (w_z, w_y). The addition of the Fermi velocity vector $\vec{v}$ takes the injection velocity vector $\vec{w}$ out of that plane. The condition for the injected particle to escape is that its radial component, w_z, should be greater than the escape velocity w_e. The plane $w_z = w_e$ thus defined cuts off a lens from the Fermi sphere. Particles with velocity vectors lying within this lens will result in Fermi jets through the receptor nucleus A_1.

Fig. 3a The number of particles jetted per collision through both nuclei, divided by the reduced mass number A_r, is plotted against a conventional variable X, proportional to the initial relative collision velocity U_o. (X is the square root of the excess of the laboratory bombarding energy over the Coulomb barrier, divided by the projectile mass number). The curve refers to head-on collisions, the circles to angular-momentum-averaged collisions for a number of systems studied experimentally.

Fig. 3b The relative velocity anomaly $\Delta v/v_{ref}$ is plotted against the same variable X as in Fig. 3a. The calculations underlying Figs. 3a and 3b are based on the analytic formulae in sec.3.

Fig. 4 A comparison of our calculations with ref. (2) for the energy spectra and angular distributions of jetted neutrons. The symbol "f" refers to "forward" jets (through the Gd target) and "f + b" to the sum of forward and backward jets.

Fig. 5 A comparison of our calculations with ref. (4). Our curves refer to results for neutrons jetted through the Nb target, scaled up by the factor (A/N). (See text.) The results of ref. (4) are shown as reported and also scaled up by a factor 2.34 to facilitate a comparison of the intrinsic shapes of the spectra.

Fig. 6 A comparison of the numerically calculated spectra of neutrons and protons (jetted through one of the partners in a symmetric reaction with A = 120, $U_o = 0.5v_F$, $\alpha = 0$) with the Gaussian parameterization described in sec. 6.

Fig. 7 The total cross section for jetting through fragment A_1 as a function of the asymmetry α defined as $(A_1 - A_2) / (A_1 + A_2)$ for various values of A and U_o. The results are for the case of no absorption.

Fig. 8 Same as Fig. 7 but with absorption included.

Fig. 9 The mean velocity $\overline{u_\parallel}$ for jetting through fragment A_1 as function of the asymmetry α, for various A and U_o. The dashed line is the result for head-on collisions, which is the limiting behavior for very heavy, fissile systems, where only small impact parameters have a chance of surviving fission. The dot-dashed lines correspond to the cut-off imposed by the threshold velocity U_c, given by $(\eta - 1)v_F$.

Fig. 10 The parallel width parameter $\Delta_\parallel$ as a function of α for various A and U_o.

Fig. 11 The transverse width parameter $\Delta_\perp$ as a function of α for various A and U_o.

Fig. 12 The dependence on U_o of the parameters $\sigma_{tot.}$, $\overline{u}_\parallel$, $\Delta_\parallel$ and $\Delta_\perp$ for proton and neutron jets through one of the fragments, for A = 120, α = 0. The calculations correspond to no absorption.

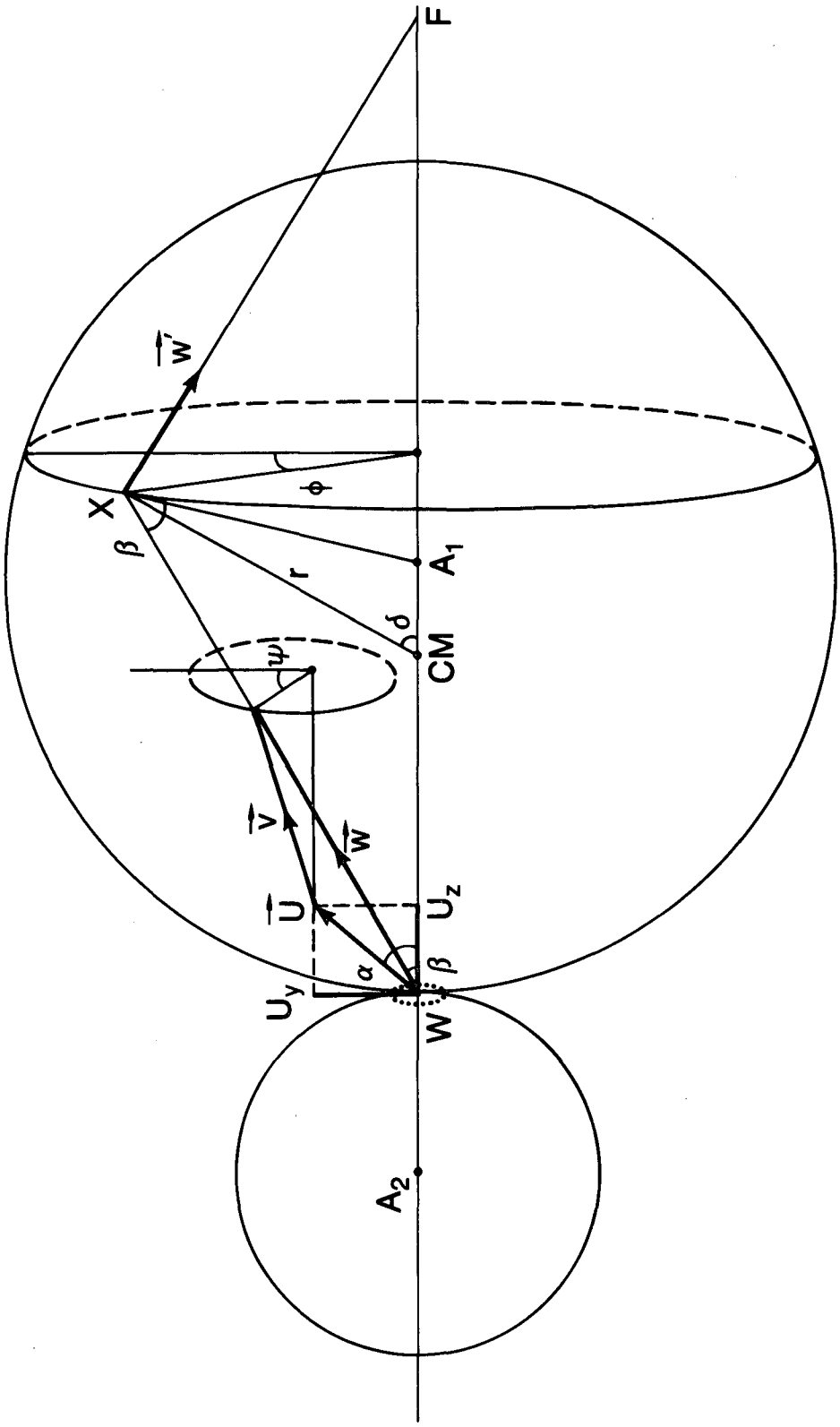

XBL 8411-6338

FIG. 1

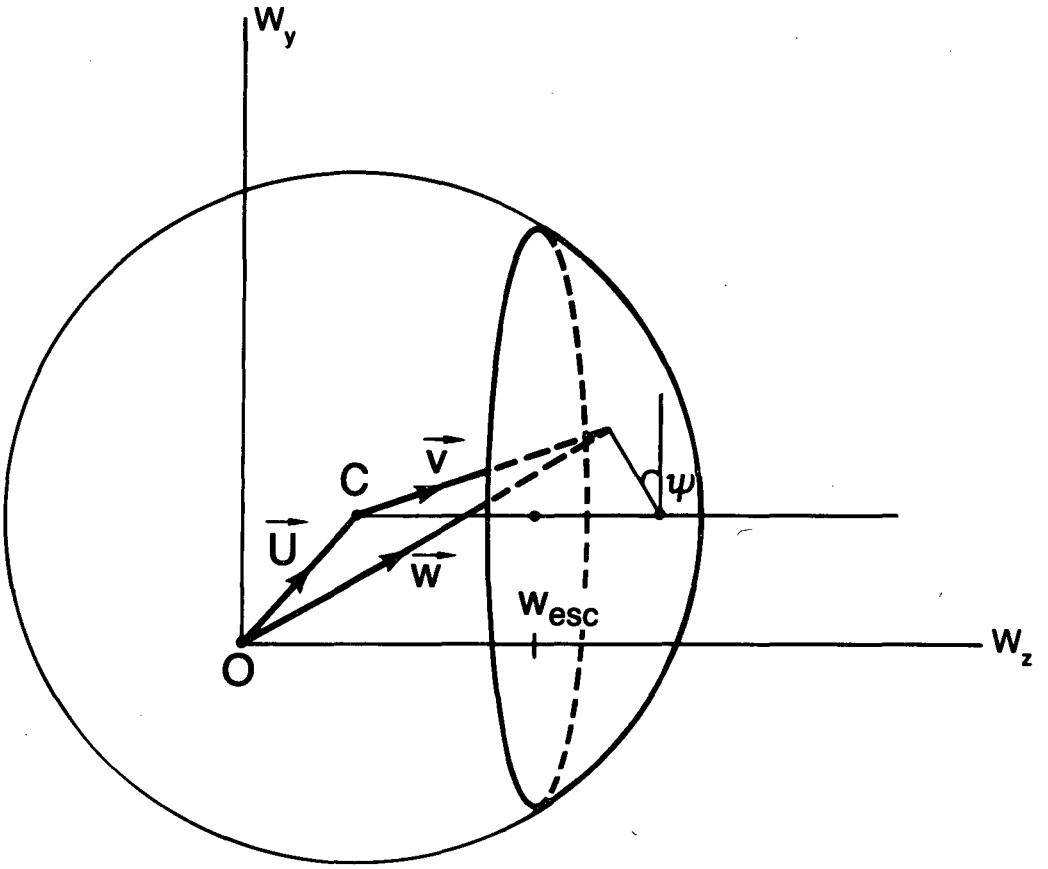

XBL 8411-6337

FIG. 2

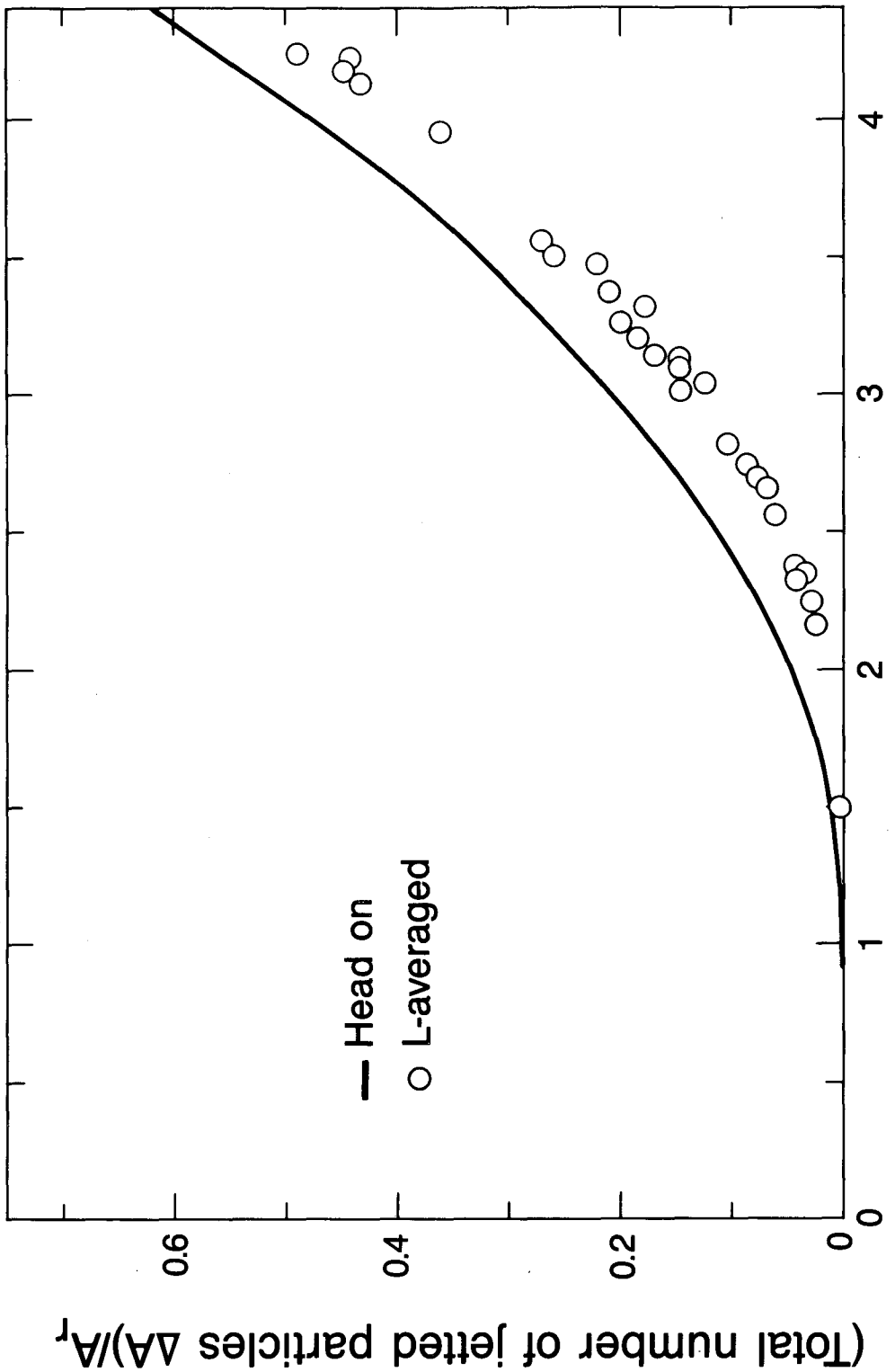
(Total number of jetted particles ΔA)/A$_r$
0
0.2
0.4
0.6
0
1
2
3
4
Head on
L-averaged
$X = \sqrt{(E - V_B)/A_p}$
XBL 842-10036

FIG. 3a

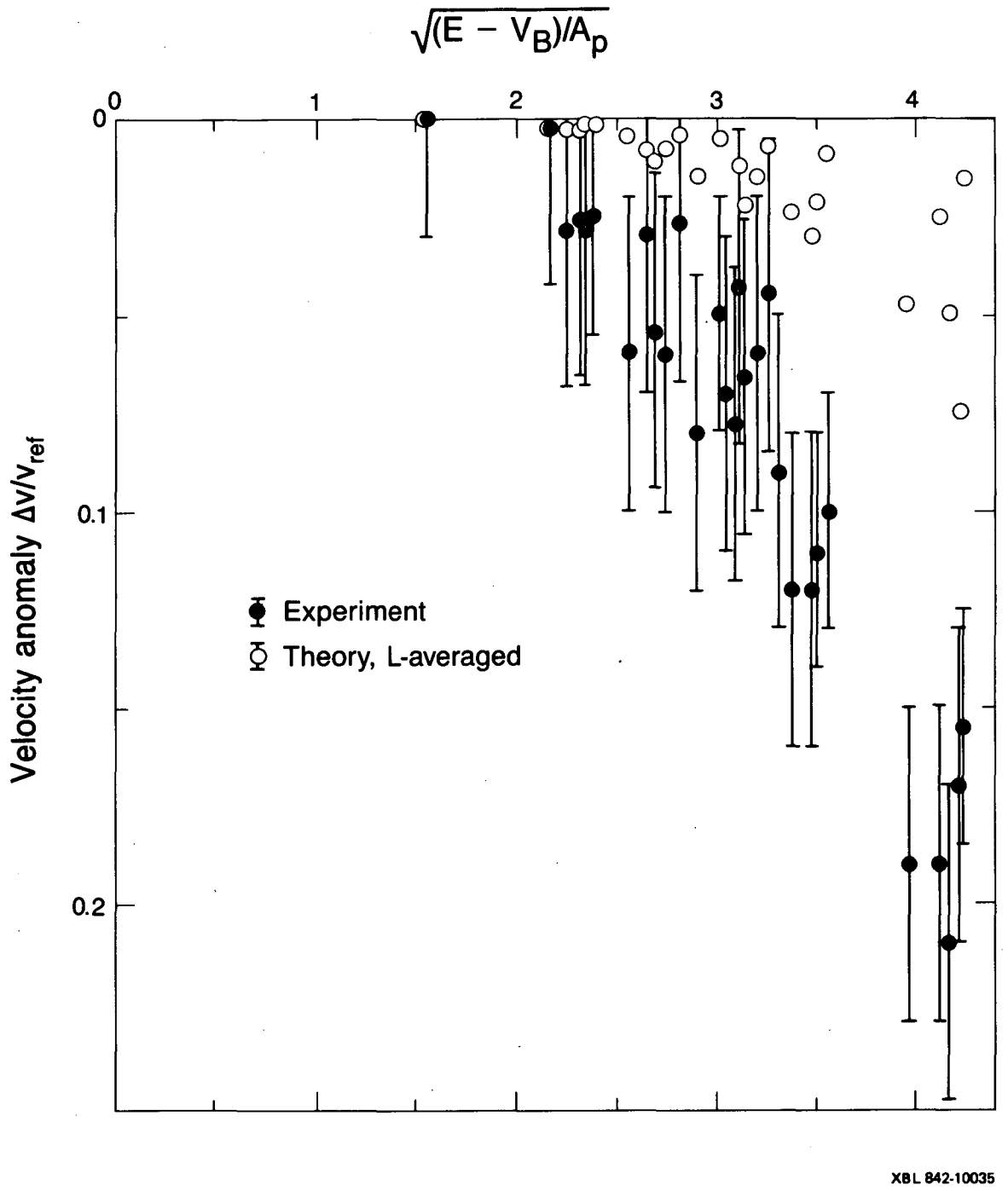
$\sqrt{(E - V_B)/A_p}$
0
1
2
3
4
0
0.1
0.2
Velocity anomaly $\Delta V/V_{ref}$
Experiment
Theory, L-averaged
XBL 842-10035

FIG. 3b

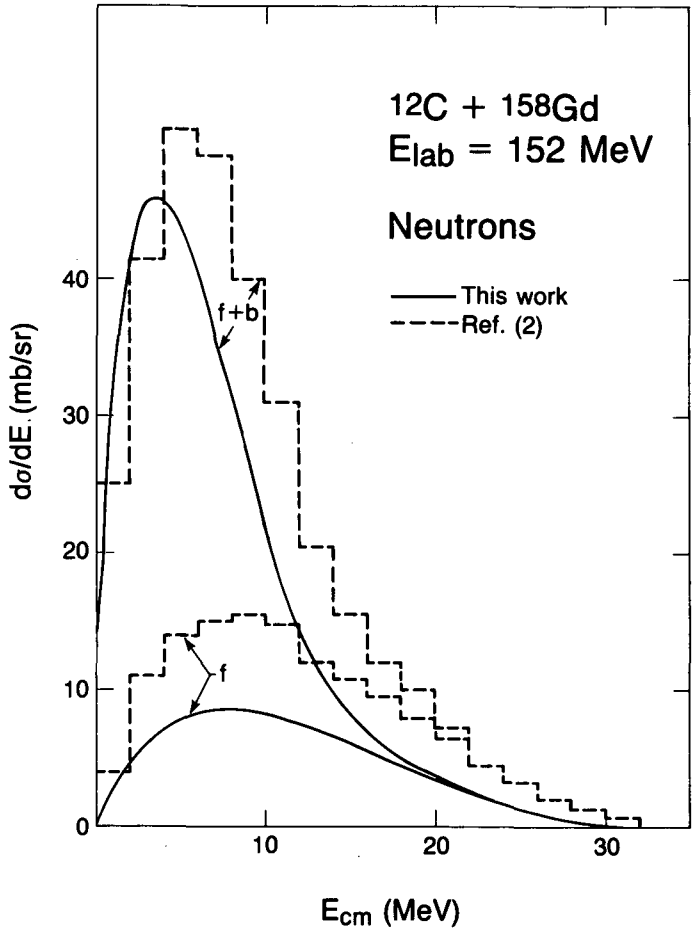

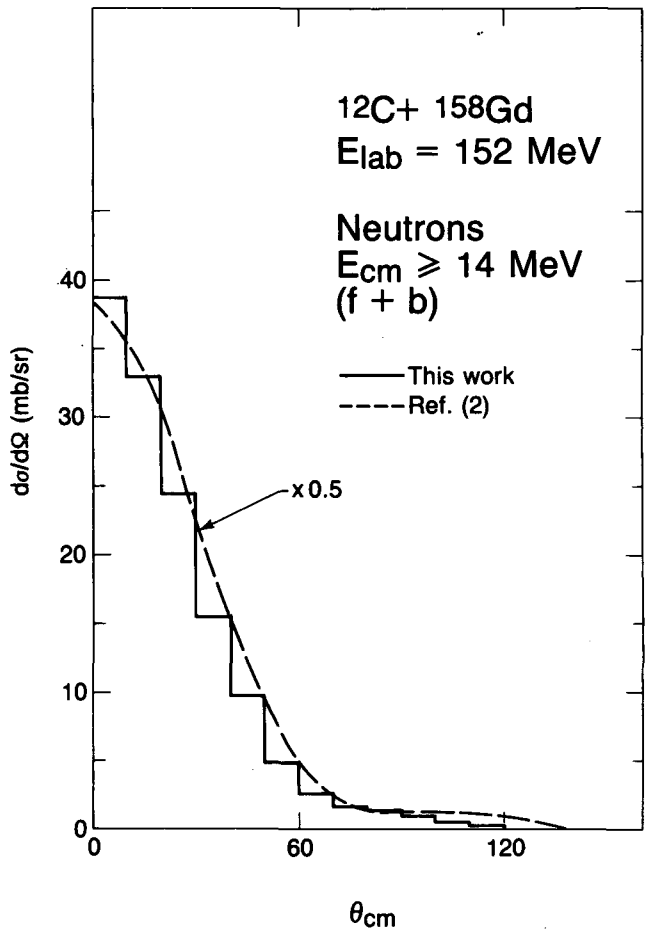

XBL 845-10540

FIG. 4

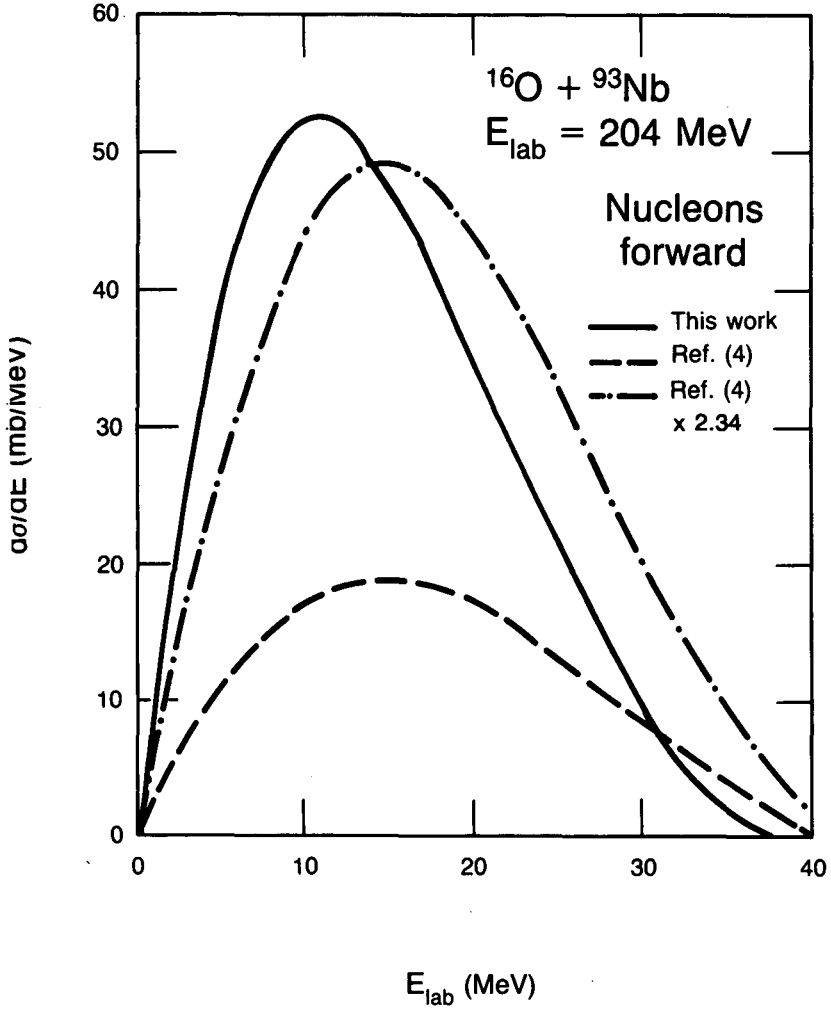

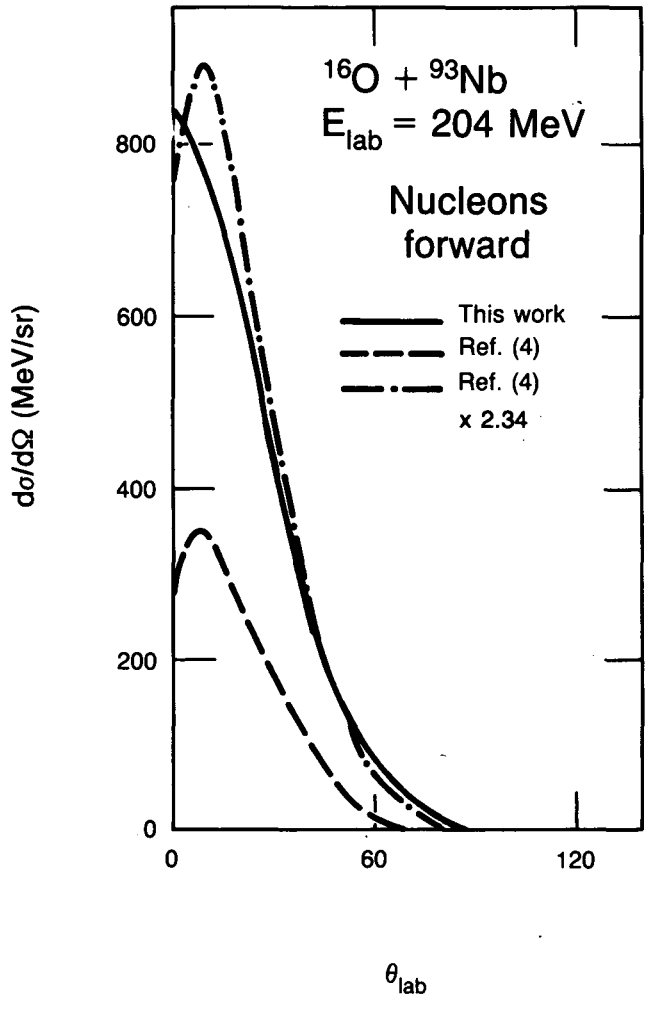

XBL 846-10679

FIG. 5

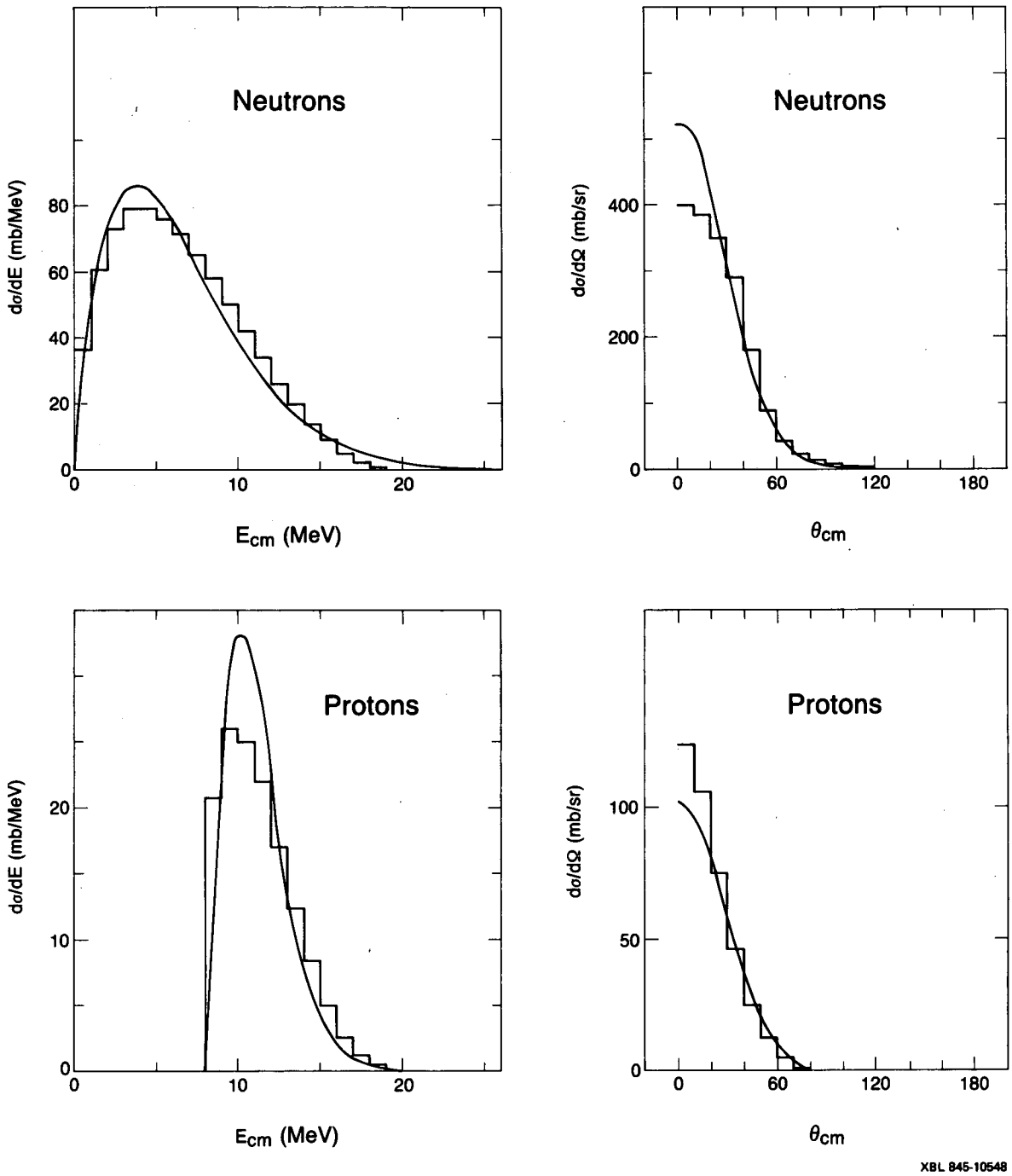
Neutrons
dσ/dE (mb/MeV)
0
20
40
60
80
0
10
20
Ecm (MeV)
Neutrons
dσ/dΩ (mb/sr)
0
200
400
0
60
120
180
θcm
Protons
dσ/dE (mb/MeV)
0
10
20
0
10
20
Ecm (MeV)
Protons
dσ/dΩ (mb/sr)
0
50
100
0
60
120
180
θcm
XBL 845-10548

FIG. 6

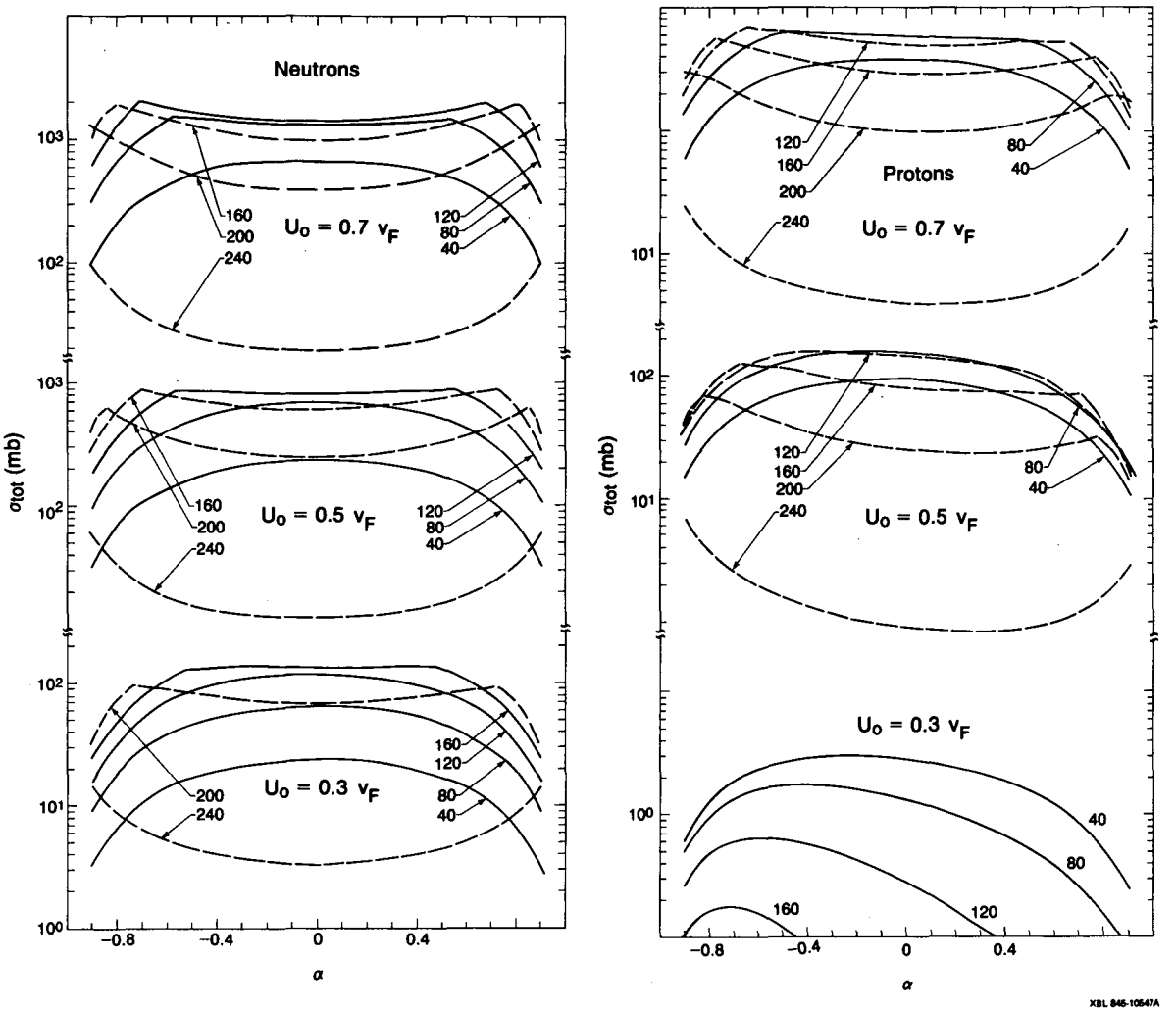
Neutrons
Protons
$U_o = 0.7\ v_F$
$U_o = 0.5\ v_F$
$U_o = 0.3\ v_F$
σ_{tot} (mb)
α
160
200
240
120
80
40
XBL 846-10547A

FIG. 7

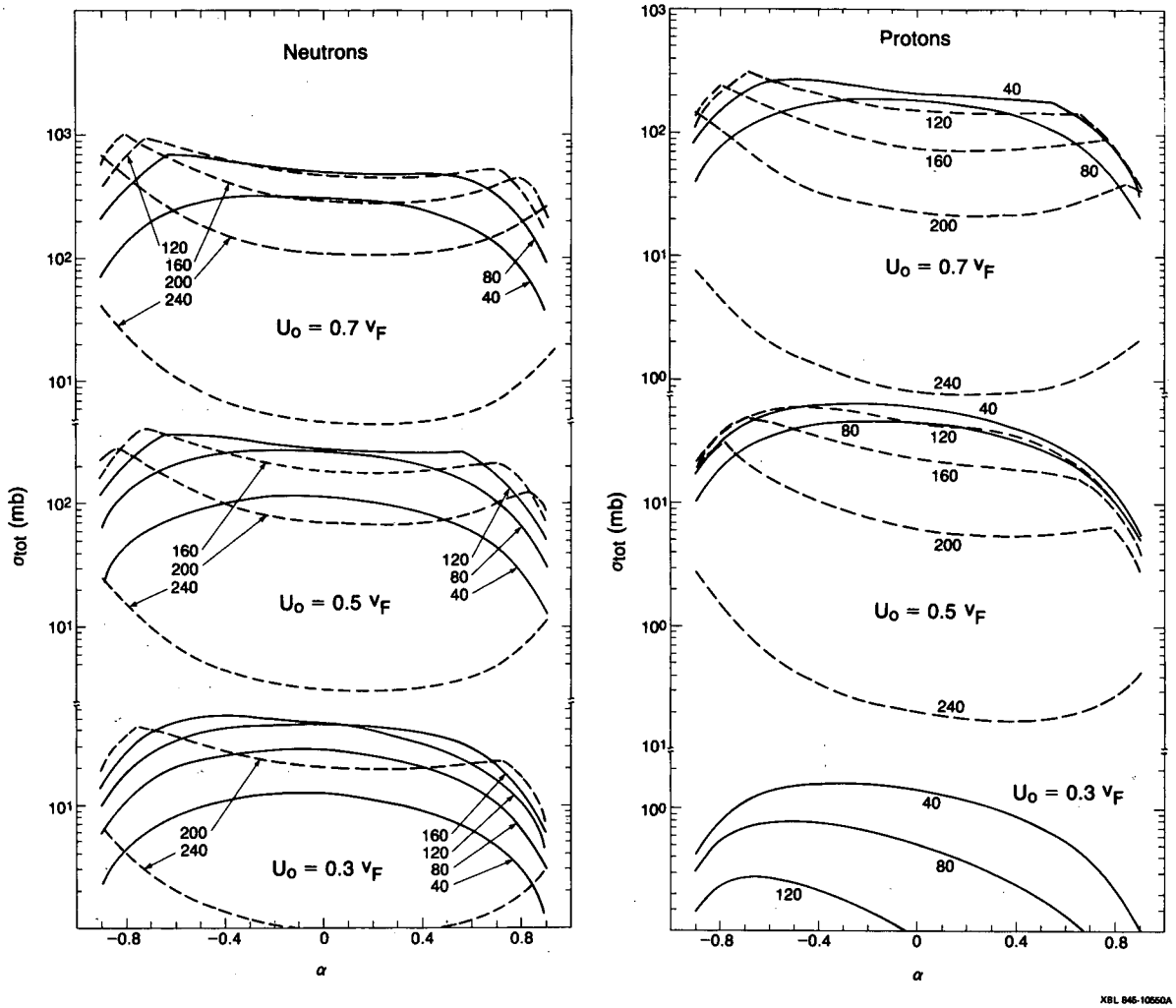
Neutrons
Protons
σ_{tot} (mb)
$U_o = 0.7\ v_F$
$U_o = 0.5\ v_F$
$U_o = 0.3\ v_F$
120
160
200
240
80
40
α
XBL 846-10550A

FIG. 8

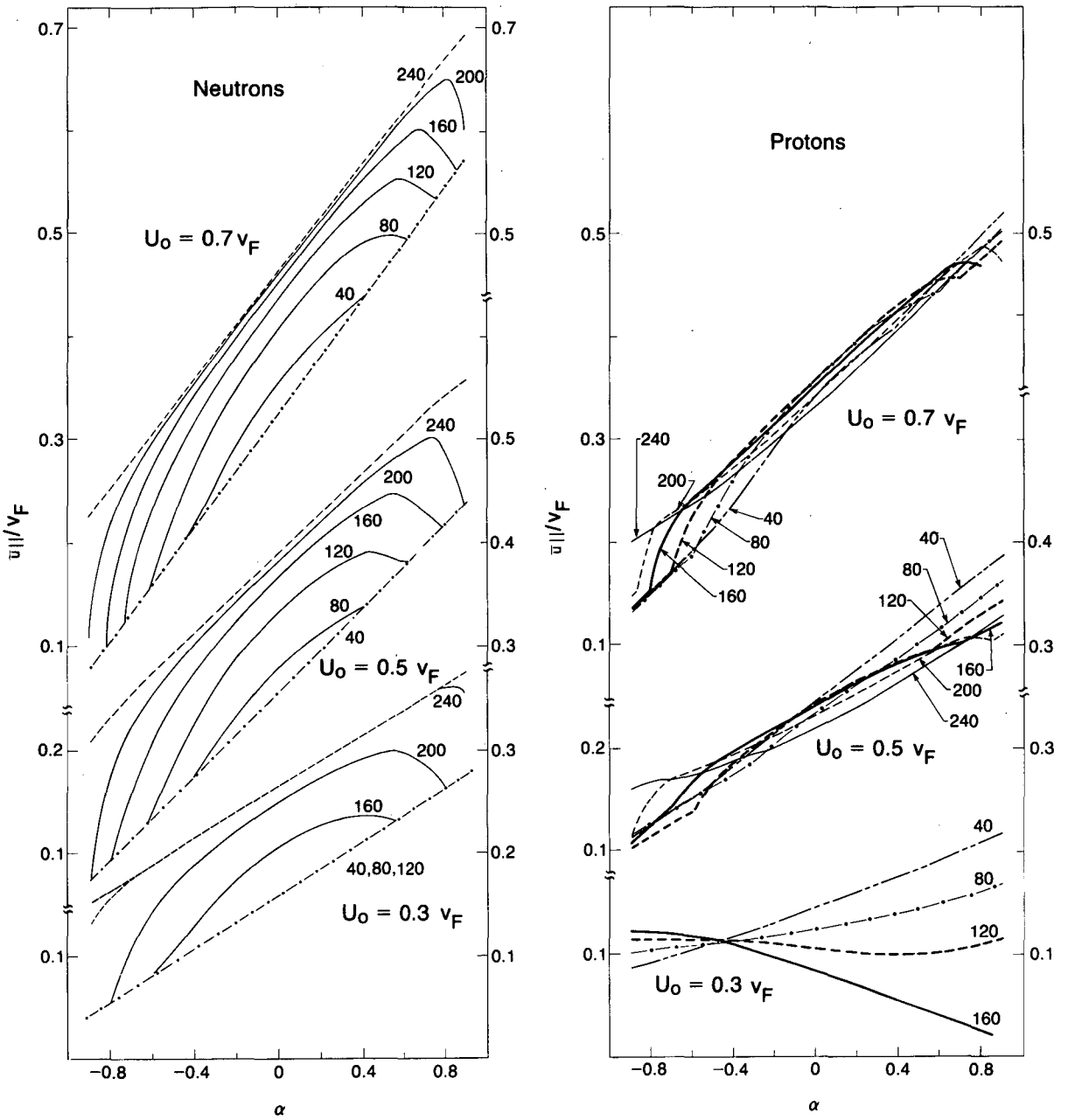

XBL 845-10541A

FIG. 9

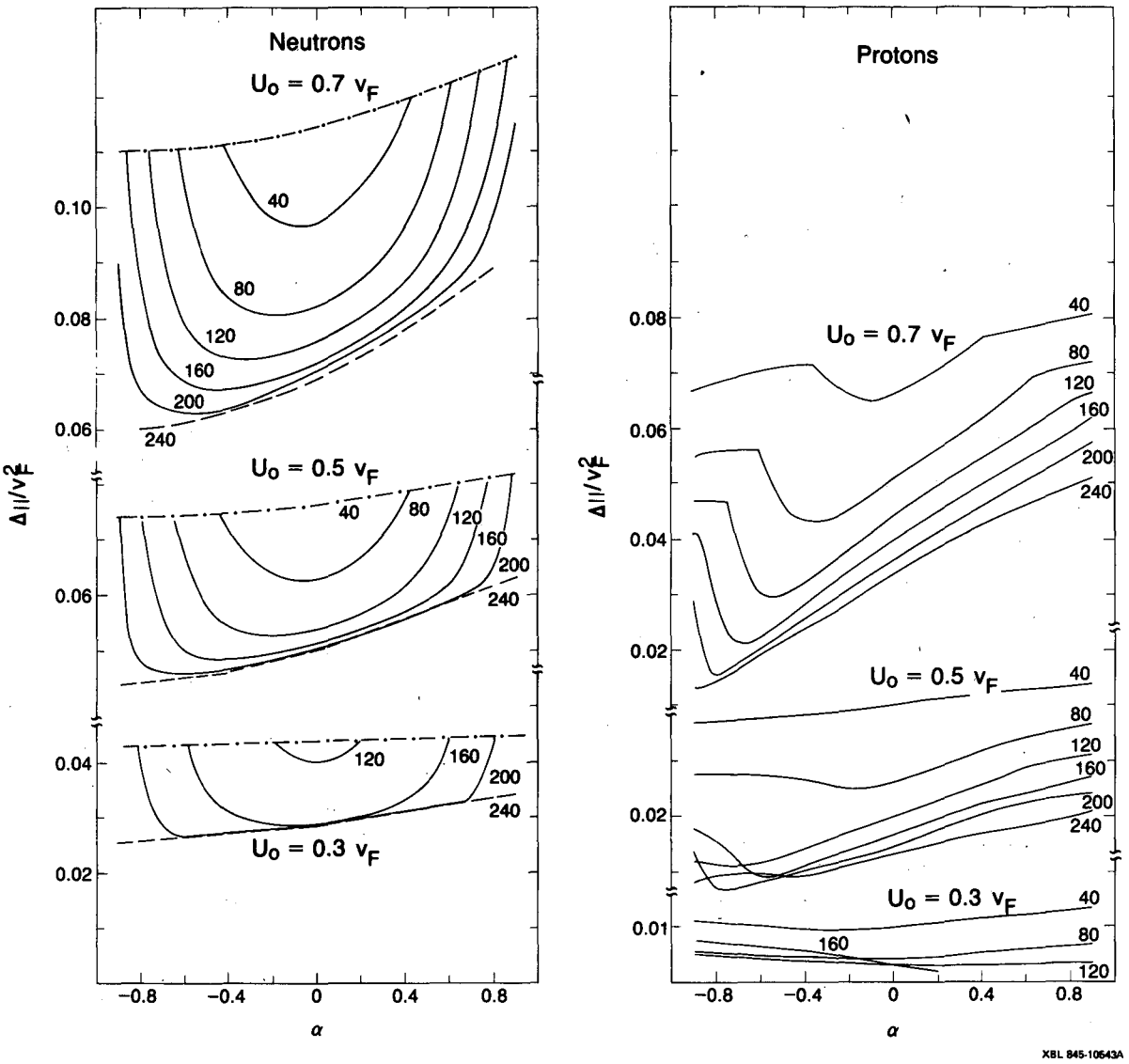
Neutrons
$U_o = 0.7\ v_F$
40
80
120
160
200
240
$U_o = 0.5\ v_F$
40
80
120
160
200
240
$U_o = 0.3\ v_F$
120
160
200
240
0.10
0.08
0.06
0.04
0.02
Δ_{11}/v_F^2
−0.8
−0.4
0
0.4
0.8
α
Protons
$U_o = 0.7\ v_F$
40
80
120
160
200
240
$U_o = 0.5\ v_F$
40
80
120
160
200
240
$U_o = 0.3\ v_F$
40
80
120
160
0.08
0.06
0.04
0.02
0.01
Δ_{11}/v_F^2
−0.8
−0.4
0
0.4
0.8
α
XBL 845-10643A

FIG. 10

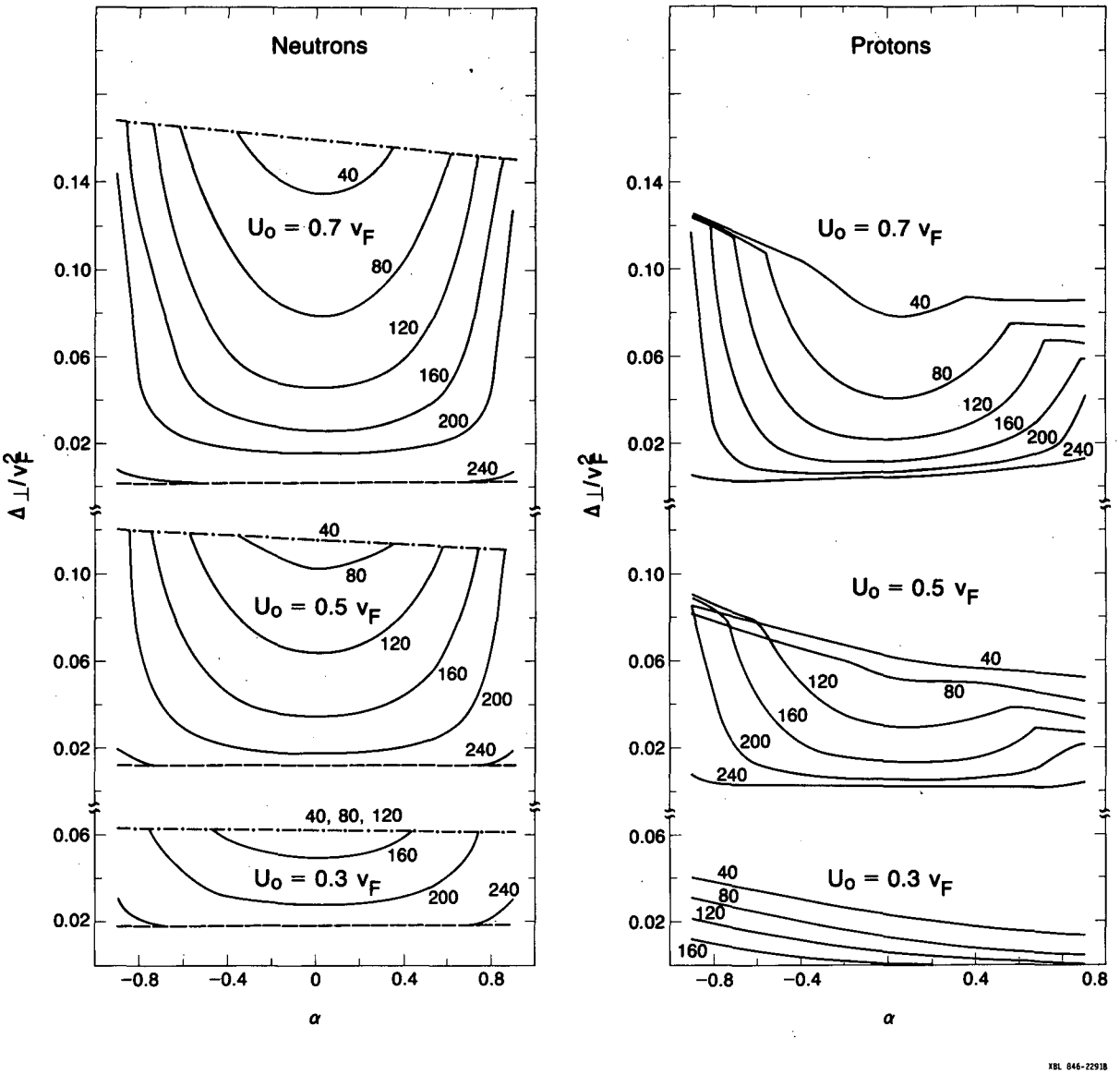
Neutrons
Protons
$U_o = 0.7\ v_F$
$U_o = 0.5\ v_F$
$U_o = 0.3\ v_F$
40
80
120
160
200
240
40, 80, 120
$\Delta_\perp / v_F^2$
α
0.14
0.10
0.06
0.02
−0.8
−0.4
0
0.4
0.8
XBL 846-2291B

FIG. 11

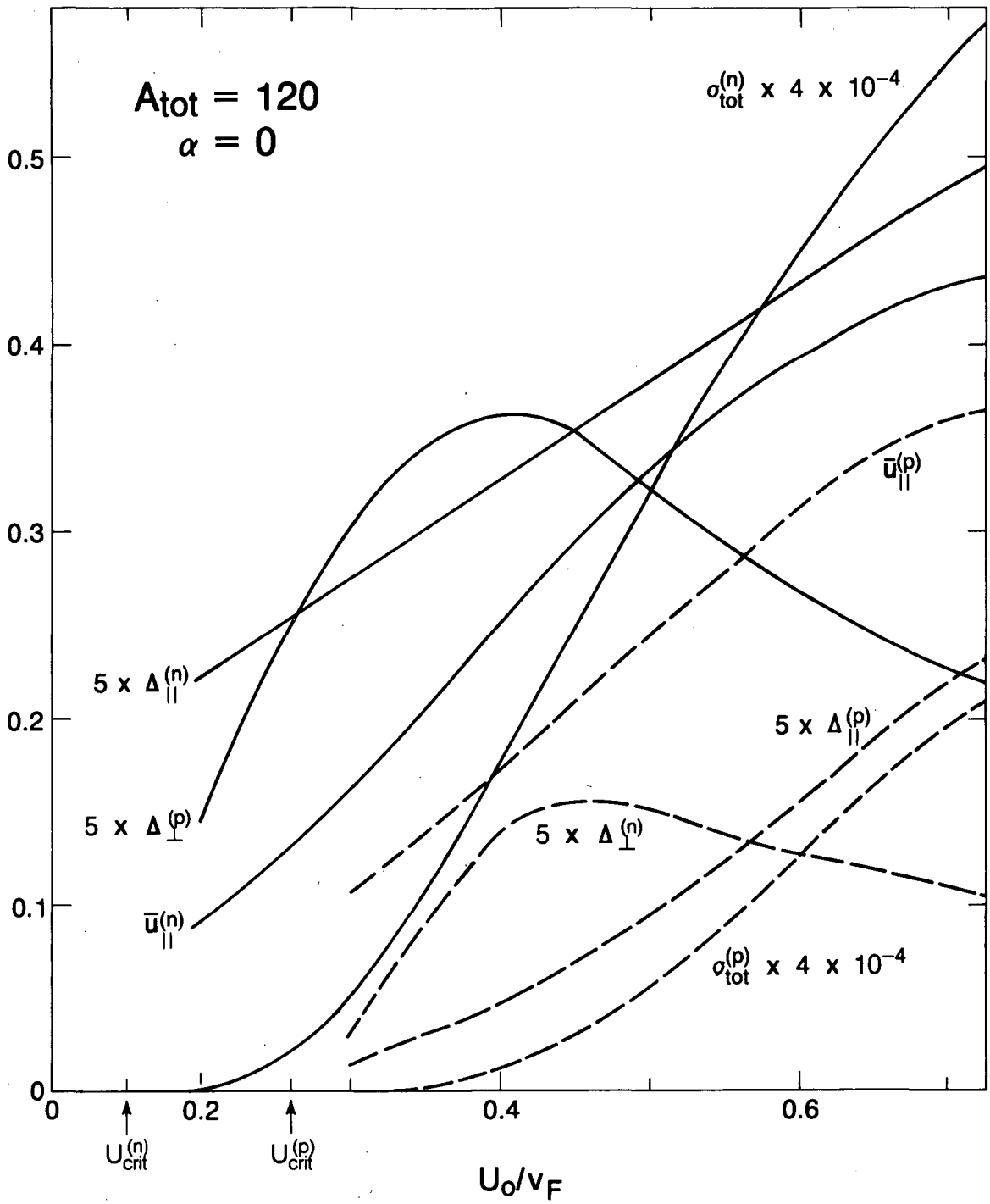

XBL 845-10539

FIG. 12

This report was done with support from the Department of Energy. Any conclusions or opinions expressed in this report represent solely those of the author(s) and not necessarily those of The Regents of the University of California, the Lawrence Berkeley Laboratory or the Department of Energy.

Reference to a company or product name does not imply approval or recommendation of the product by the University of California or the U.S. Department of Energy to the exclusion of others that may be suitable.

TECHNICAL INFORMATION DEPARTMENT
LAWRENCE BERKELEY LABORATORY
UNIVERSITY OF CALIFORNIA
BERKELEY, CALIFORNIA 94720